Metabolism and hypoxia tolerance of the endangered white abalone (*Haliotis sorenseni)*: Implications for conservation and restoration efforts

Stephanie J. Fan[a,b], Taylor R. Smith[c], Nasseer Idrisi[d], John R. Hyde[e], Nicholas C. Wegner[e,*]

[a] Department of Environmental and Ocean Sciences, University of San Diego, 5998 Alcalá Park, San Diego, CA 92110, USA

[b] Ocean Associates, under contract to: Fisheries Resources Division, Southwest Fisheries Science Center, National Marine Fisheries Service, National Oceanic and Atmospheric Administration, 8901 La Jolla Shores Dr, La Jolla, CA 92037, USA

[c] Department of Biological Sciences, California State University Long Beach, 1250 Bellflower Boulevard, Long Beach CA 90840, USA

[d] California Department of Water Resources, 78078 Country Club Dr., Ste 109, Bermuda Dunes, CA 92203, USA

[e] Fisheries Resources Division, Southwest Fisheries Science Center, National Marine Fisheries Service, National Oceanic and Atmospheric Administration, 8901 La Jolla Shores Dr., La Jolla, CA 92037, USA

*Corresponding author:
Email: nick.wegner@noaa.gov
Phone: 858-546-7080
Fax: 858-546-7003

Abstract

The white abalone, *Haliotis sorenseni*, is an endangered marine gastropod that has shown no signs of population recovery despite fishery closure and protective status. To better understand the energetic demands, hypoxia tolerance, and critical habitat of this species, we measured oxygen consumption rates over a size range of captive-reared *H. sorenseni* at different environmental oxygen concentrations and temperatures in comparison to the more common red abalone, *H. rufescens*. We found that *H. sorenseni* has a relatively low metabolic rate that likely contributes to generally slow growth that can hamper recovery efforts. We also discovered that both *H. sorenseni* and *H. rufescens* appear to partially conform to ambient oxygen conditions by lowering their metabolism to deal with increasing hypoxia while still retaining an aerobic scope until reaching a critical oxygen concentration (P_{crit}), at which point they become oxylimited. For species exhibiting such relationships, determining the P_{90}, P_{75}, P_{50}, and P_{25} (dissolved oxygen value at which oxygen consumption is 90%, 75%, 50%, and 25% of resting metabolic rate), as well as the P_{crit} and oxygen supply capacity, are useful metrics to compare hypoxia sensitivities among species and individuals. Variability in these metrics suggest potential fitness differences for *H. sorenseni* individuals spawned and raised in captivity for restoration outplanting. Higher temperatures also led to an increase in P_{90}, P_{75}, P_{50}, P_{25}, and P_{crit} and decrease in factorial aerobic scope for *H. sorenseni,* revealing the potential compounding effects of high temperature and low oxygen. Our results thus provide a suite of physiological metrics on which to test the health and fitness of captive-reared abalone and can help inform selection of appropriate outplanting sites for endangered *H. sorenseni*.

Keywords: critical oxygen level, invertebrate, metabolic scaling, oxyconformer, oxyregulator, respiration, temperature

1. Introduction

In 2001, the white abalone, *Haliotis sorenseni*, was the first marine invertebrate to be listed as endangered by the United States under the Endangered Species Act (Federal Register 66 FR 29046). The collapse of the species resulted from serial depletion through overfishing and inadequate fishery regulations, and was likely compounded by disease (Davis *et al.*, 1996, Karpov *et al.*, 2000, Hobday *et al.*, 2001). Like other abalone species, the white abalone is a broadcast spawner, and spawning individuals need to be in close proximity (less than 3 m apart) for successful fertilization, suggesting that white abalone densities less than approximately 2,000 abalone ha^{-1} are not sustainable (NMFS, 2008, Stierhoff *et al.*, 2012). Unfortunately, estimates based off the most recent surveys suggest densities well below this threshold at <1 abalone ha^{-1}, and there has been minimal evidence of successful *H. sorenseni* recruitment since the 1990s (Stierhoff *et al.*, 2014, Catton *et al.*, 2016, DiNardo *et al.*, 2021). Thus, even despite the closure of the white abalone fishery in 1996 and its listing as federally "Endangered" in 2001, *H. sorenseni* has not shown signs of natural recovery, and the number of surviving wild white abalone continues to decline as the remaining isolated adults age.

In response, the White Abalone Recovery Consortium comprised of various academic institutions, state and federal government entities, commercial abalone growers, and non-government organizations (e.g., public aquaria) was formed to help recover the species through continued assessment of wild populations, spawning and rearing white abalone in captivity, and outplanting captive-bred abalone back into the wild (Rogers-Bennett *et al.*, 2016). Since the start of this recovery program, thousands of *H. sorenseni* have been successfully reared in captivity, and outplanting operations began in 2019. However, because of their historically low biomass (the pristine population size of *H. sorenseni* in California was estimated at about 360,000

individuals) and fast exploitation rate (the boom and bust of the *H. sorenseni* fishery is thought to have occurred in just a few years from 1969-1977), little is known about their preferred habitat and environmental tolerances, which have important implications for selecting sites for outplanting (Karpov *et al*., 2000, Hobday *et al*., 2001, Rogers-Bennett *et al.*, 2002, DiNardo *et al*., 2021).

H. sorenseni is the deepest dwelling abalone species on the west coast of the United States, being found most abundantly at depths of 20-60 m, often near the lower margins of kelp forests (Davis *et al*., 1996, Butler *et al.*, 2006). Such habitat is vulnerable to intermittent exposure to local upwelling with cold, hypoxic water that can negatively affect coastal marine organisms (Grantham *et al.*, 2004, Vaquer-Sunyer and Duarte, 2008, Frieder *et al.*, 2012, Boch *et al.*, 2018, Kekuewa *et al.*, 2022). As a benthic gastropod with limited mobility, *H. sorenseni* likely has limited ability to actively avoid the adverse effects of hypoxic upwelling (Parnell *et al.*, 2020). This is particularly concerning in that hypoxia has been shown to decrease both the growth and survivorship of several abalone species (Harris *et al.*, 1999, Kim *et al.*, 2013, Morash and Alter, 2016, Calderón-Liévanos *et al.*, 2019, Nam *et al.*, 2020, Shen *et al.*, 2020, Shen *et al.*, 2022), and changes to abalone metabolism and growth can occur with even slight reductions in environmental dissolved oxygen in some species (Jan and Chang, 1983, Gaty and Wilson, 1986, Harris *et al.*, 1999). Despite being one of the deepest dwelling abalone and most likely to regularly encounter hypoxia, little is known about the physiological response of *H. sorenseni* to low environmental oxygen.

Here we examined basic metabolic parameters and the hypoxia tolerance of *H. sorenseni* by assessing the effects of graded reductions in environmental dissolved oxygen on the rate of oxygen consumption using closed respirometry techniques. Specifically, understanding the

effects of reduced environmental oxygen on oxygen consumption (a proxy for metabolic rate), provides insight into how metabolically-expensive processes such as internal ion balance, predator avoidance, growth, and reproduction may be affected by suboptimal dissolved oxygen levels. In addition, metabolic parameters were made over a range of body sizes and at two temperatures (11°C and 15°C – representing the mean seasonal temperature range encountered in deep kelp forest habitat where white abalone are currently being outplanted) to assess the impacts of abalone size and environmental temperature. Such metabolic data are valuable in identifying 1) potentially suboptimal dissolved oxygen levels and temperatures, and 2) abalone sizes or life stages that may be more or less hypoxia tolerant, both of which can help inform outplanting decisions and restoration efforts for the species. Measures of white abalone metabolic parameters and hypoxia tolerance were made in comparison to red abalone, *H. rufescens,* another abalone species that often inhabits overlapping temperatures and depths with *H. sorenseni* in southern California, but exhibits faster growth rates and has proved more resilient to population decline associated with overfishing and disease.

2. Materials and methods

2.1. Abalone husbandry

H. sorenseni (n = 29, 4.6 – 103.3 g, 34.8 – 91.5 mm in length) examined in this study were raised from larvae produced by the White Abalone Recovery Consortium from three different cohorts. *H. rufescens* (n = 29, 7.7 – 103.3 g, 39.1 – 94.0 mm) were derived from larvae from two cohorts, one from the Cultured Abalone Farm (Goleta, CA) and one from the Abalone Farm (Cayucos, CA). Abalone were reared in long-term culture tanks with temperature-controlled filtered seawater and fed ad libitum a variety of brown algae (mostly giant kelp,

Macrocystis pyrifera) harvested locally, as well as dulse, *Palmaria mollis,* grown onsite. Abalone were tagged for identification with flexible shellfish tags (FT-LF-97, $^{1}/_{8}$ x ¼", Floy Tag & Mfg., Inc., Seattle, WA) using a cyanoacrylate adhesive (CorAffix, Two Little Fishies Inc., Miami Gardens, FL). All abalone husbandry and experimentation were performed in accordance with SWFSC Animal Care and Use Committee Protocol #SW1702 and ESA permit #14344-2R.

2.2 Respirometry trials to determine metabolic parameters and hypoxia tolerance

Respirometry experiments were performed to examine the effects of environmental oxygen on abalone oxygen consumption (a proxy for metabolic rate) in order to better understand the hypoxia tolerance of *H. sorenseni* over a potential size range for outplanting (~30-100 mm) in comparison to *H. rufescens*. Prior to experimentation, each abalone was gently dislodged from its home tank by inserting a plastic spatula or card under the foot. The abalone was then placed on a 6.7 mm thick PVC disk (57, 77, or 95 mm in diameter depending on abalone size), surrounded by fine mesh netting, and suspended in a holding tank to fast the animal for a minimum of 48 h prior to respirometry measurements. Following the fasting period, the abalone (attached to the PVC disk) was transferred from the holding tank to the respirometer via a plastic beaker, which allowed the abalone to remain submerged in seawater and attached to its substrate in order to minimize handling stress and prevent the introduction of air bubbles under the shell and into the respirometry system.

The respirometer consisted of a cylindrical acrylic holding chamber and a recirculating loop composed of flexible plastic polymer tubing, a small pump (Brushless DC pump, 12V; ZKSJ; Shenzhen, China), two sensor ports (for dissolved oxygen and temperature sensors), and two 3-way stopcocks (to allow for opening and closing the system to the surrounding

temperature-controlled buffer-tank water) (Fig. S1). The abalone holding chamber (62 x 25 mm, 80 x 30 mm, or 100 x 40 mm; inner diameter x inner height; Loligo Systems; Tjele, Denmark) was matched to the size of the abalone and corresponding PVC disk size in order to minimize the water volume within the respirometer to enhance the oxygen consumption signal. Once placed in the respirometer, an abalone was given a one-hour acclimation period, following which the 3-way stopcocks were closed to isolate the respirometer from the surrounding buffer tank for oxygen consumption measurements. Longer acclimations times (e.g., overnight or several days) were not used as preliminary trials showed that longer acclimation did not result in lower resting oxygen consumption rates (Fig. S2A) and led to an increased bacterial load within the respirometer, which increased the background respiration rate. The abalone's respiration caused the system to become progressively hypoxic over time, allowing resting oxygen consumption rate to be monitored until the oxygen level reached approximately 5-10% air saturation. Oxygen level and temperature (°C) were monitored with a fiber optic oxygen probe and a temperature sensor connected to either a Fibox 3 system (PreSens Precision Sensing; Regensburg, Germany), which could monitor one abalone respirometer at a time, or a Witrox 4 oxygen meter system (Loligo Systems; Viborg, Denmark) that could monitor up to four abalone respirometers at once. Following completion of the respirometry trial, the abalone was removed from both the chamber and PVC disk to measure its mass, length, and volume (abalone volume was measured via displacement in a graduated cylinder). The respirometry system was flushed for at least 15 minutes and then resealed with the PVC disk inside, but without the abalone, for a minimum of one hour to obtain measurements of background bacterial respiration.

Respirometry experiments were first conducted for all abalone at 15°C. In order to examine the effects of temperature on metabolism and hypoxia tolerance, respirometry trials

were repeated at 11°C on a subset of each species from the middle of the examined body-size range (*H. sorenseni*, 24.4 - 50.5 g, n = 10; *H. rufescens*, 21.7 – 35.2 g, n = 12). Temperatures of 15°C and 11°C were chosen as these temperatures represent approximate mean seasonal (summer vs winter) temperatures encountered in deep kelp forest habitat in the Southern California Bight where both species can be found (Frieder *et al*., 2012). Abalone were acclimated to their experimental temperature for at least 30 days prior to respirometry trials.

2.3. Data analysis for metabolic and hypoxia tolerance parameters

For each respirometry trial, abalone oxygen consumption rate (M_{O_2} in mg O_2 h^{-1}) was determined over 5% oxygen saturation intervals (e.g., the mean M_{O_2} was calculated when the dissolved oxygen level of the respirometer was between 95-100% air saturation, 90-95% saturation, down to 5-10% saturation (Fig. 1). This analysis method was chosen based on preliminary data showing near immediate reductions in abalone M_{O_2} with declining environmental oxygen (e.g., Fig. S2B) and based on similar previous analyses for other abalone species (Jan and Chang, 1983, Harris *et al*., 1999). The relationship of abalone M_{O_2} versus environmental oxygen level displayed as either a logarithmic or linear function (compare Figs. 1A and 1B), and the best-fit model was chosen for each individual using an ordinary least squares analysis via lm() function in base R package v4.4.1 (R Core Team, 2024). Preliminary model fitting of this relationship between M_{O_2} and environmental oxygen level occasionally revealed rare outlier points (e.g., abnormally high or low M_{O_2} values, defined here as greater than 30% different than the predicted value of the best-fit function; outliers comprised less than 2% of the data). These outliers, which were likely associated with abalone activity within the chamber, were removed and the modeled function was refit. Resting M_{O_2}, a proxy for resting

197 metabolic rate (RMR), was estimated using the best-fit function for each individual abalone at
198 100% air saturation (=P_{100}) (Fig. 1), which supplementary trials showed was similar to the $q_{0.25}$
199 of M_{O_2} measurements over several days (Fig. S2C) and thus a good estimation of RMR (Chabot
200 *et al*., 2016; Reemeyer & Rees, 2019). The P_{90}, P_{75}, P_{50}, and P_{25} (dissolved oxygen level at
201 which oxygen consumption was 90%, 75%, 50%, and 25% of RMR) were also estimated using
202 the best-fit functions as shown in Figure 1. The oxygen supply capacity (α in $mgO_2\ h^{-1}\ \%O_2^{-1}$)
203 was calculated as the maximum rate of oxygen uptake per 5% oxygen bin (Fig. 1C,D), which
204 was used to estimate the P_{crit} and theoretical maximum metabolic rate (MMR) and aerobic scope
205 (Fig. 1E,F) (Seibel and Deutsch, 2020, Seibel *et al*., 2021). Comparison of multi-day
206 respirometry data (Fig. S2A) with progressive hypoxia curves (Fig. S2B) showed the oxygen
207 supply capacity accurately predicted the maximum metabolic rate of abalone observed over the
208 course of five days in the respirometer (Fig. S2C). Likewise, examination of rare elevated M_{O_2}
209 outliers for individual abalone across varying dissolved oxygen levels showed good agreement
210 with the oxygen supply capacity (Fig. S3). P_{crit} was estimated where the difference between the
211 oxygen supply capacity and oxygen consumption curve was lowest (approximate intersection –
212 see Fig. 1E,F).

213 The relationship of resting oxygen consumption with total body mass (including the mass
214 of the shell) was determined according to the power-law equation:

215 $$M_{O_2} = aM^b \quad (1)$$

216 Where M_{O_2} is the oxygen consumption rate, a is the oxygen consumption rate intercept at a mass
217 of 1 g, M is mass in grams, and b is the mass scaling exponent or allometric slope. Because the
218 shell is not metabolically active, the relationship of M_{O_2} with just the wet tissue mass (excluding
219 the shell) was also estimated. This was estimated using data on shell and wet tissue mass from

96 *H. sorenseni* (0.5 – 37.6 g, 13.6 – 64.4 mm in length) and 533 *H. rufescens* (42.0 – 237.4 g, 70.0 – 115.0 mm in length) that were measured for unrelated work (J. Moore, California Department of Fish and Wildlife, unpublished data). These data showed the ratio of wet tissue mass to total body mass (including the shell) was 0.683 ± 0.054 for *H. sorenseni* and 0.711 ± 0.049 for *H. rufescens*. This ratio did not change with body size for either species.

The Q_{10}, the factor by which oxygen consumption increases with a 10°C temperature change, was calculated according to the equation:

$$Q_{10} = \left(\frac{M_{O_2(2)}}{M_{O_2(1)}}\right)^{\left(\frac{10}{T_2 - T_1}\right)} \quad (2)$$

where $M_{O_2(1)}$ and $M_{O_2(2)}$ represent oxygen consumption rates at T_1 (11°C) and T_2 (15°C) respectively. In order to account for differences in body size between the 11 and 15°C trials, the M_{O_2} of each individual abalone was scaled to a mass of 40 g (the approximate mean mass of abalone sampled) using the species-specific mass scaling coefficients calculated in Equation 1.

2.4. Statistical analyses

Statistical analyses were completed using R v4.4.1 (R Core Team, 2024). Means are presented as ± standard deviation unless otherwise indicated. When testing the various respirometry parameters (RMR, α, MMR, factorial aerobic scope, P_{90}, P_{75}, P_{50}, P_{25}, P_{crit}) for significant differences between species at 15°C, assumptions of normality and homogeneity were assessed using a Shapiro-Wilk test and Bartlett's test. Normally-distributed and homogeneous data were analyzed using a t test, while non-normally distributed and homogeneous datasets were tested using a non-parametric Wilcoxon test. Likewise, for the subset of abalone examined at both 11 and 15 °C, metabolic and hypoxia tolerance parameters were examined using either a paired t test (if normality and homogeneity assumptions were met) or a paired samples Wilcoxon

test (if assumptions were not met) to find differences within each species at each temperature. Significant differences in the Q_{10} between species were tested using a Wilcoxon test.

For metabolic scaling data, a bootstrap regression analysis (10,000 replicates with replacement) (Frank *et al.*, 2021) was used to determine if the relationship between RMR (mg O_2 h^{-1} at 100% environmental oxygen level) and body mass differed between white and red abalone. Significant difference in RMR between species was determined if < 5% of the bootstrap regressions intersected over the range of body masses being compared. This bootstrap regression analysis was also used to assess if white and red abalone M_{O_2}(mg O_2 h^{-1}) differed significantly over the environmental dissolved oxygen level (% air saturation) range examined.

3. Results

3.1. Metabolic parameters

The relationships between resting metabolic rate (mg O_2 h^{-1}) and total body mass (including the shell) for *H. sorenseni* and *H. rufescens* are shown in Figure 2. Bootstrap analysis revealed that *H. sorenseni* had significantly lower resting metabolic rates than *H. rufescens* for the entire overlapping body mass range tested (7.7 to 103.3 g). When considering just the metabolically active tissue (e.g., total mass – shell mass), RMR for *H. rufescens* was also significantly higher than that of *H. sorenseni* for the entire overlapping tissue mass range (5.5 to 70.5 g) (Fig. S4). Likewise, when RMR for each individual was scaled to a common mass of 40 g using species-specific scaling equations determined in Fig. 2, *H. sorenseni* RMR (0.928 ± 0.186 mgO_2 h^{-1}) was significantly lower than that of *H. rufescens* (1.483 ± 0.218 mgO_2 h^{-1}) (t test, t =10.42, df =54.59, P <0.001; Table 1). Estimates of α and MMR were also significantly lower in *H. sorenseni* in comparison to *H. rufescens* (t test; t = 7.76, df = 53.29, P < 0.001),

while factorial aerobic scopes were similar between the species (t test, $t = 0.09$, df = 39.53, $P = 0.926$; Table 1).

3.2. Hypoxia tolerance

Representative graphs showing the relationship between individual abalone M_{O_2} and environmental oxygen (% saturation) are shown in Figure 1. For most individuals from both abalone species, M_{O_2} showed a logarithmic relationship with environmental oxygen, with M_{O_2} decreasing faster at lower oxygen concentrations (Fig. 1A). Specifically, a logarithmic relationship between oxygen consumption and dissolved oxygen level was observed in 24 of 29 *H. sorenseni* and all 29 *H. rufescens* when examined at 15°C. For five of the 29 white abalone trials, the M_{O_2} profiles more accurately displayed as a linear relationship (Fig. 1B) with M_{O_2} decreasing faster at higher environmental oxygen concentrations than under a logarithmic curve. When data for all individuals were standardized to a common mass and combined, this relationship presented as a logarithmic curve for both *H. sorenseni* and *H. rufescens* (Fig. 3). Bootstrap analysis revealed that the mean M_{O_2} for *H. rufescens* was significantly higher ($P < 0.05$) than that of *H. sorenseni* across the entire environmental dissolved oxygen range (Fig. 3).

Mean P_{90}, P_{75}, P_{50}, P_{25}, and P_{crit} values were determined for each species based on individual M_{O_2} vs dissolved oxygen curves (Table 1, Fig. 1, S5). Mean P_{90}, P_{75}, P_{50}, and P_{25} values were not significantly different between *H. sorenseni* and *H. rufescens* (Wilcoxon test, $W = 465$, $P = 0.497$). However, *H. sorenseni* showed greater P_{90}, P_{75}, P_{50}, and P_{25} variability, having higher outliers associated with the linear M_{O_2} functions of some individuals (Figs. 1, S5). Mean P_{crit} was also not significantly different between *H. sorenseni* and *H. rufescens* (Wilcoxon Test, $W = 346$, $P = 0.342$). In order to examine how abalone size potentially influences hypoxia

tolerance, P_{50} values for both abalone species were graphed in relation to abalone shell length, a common metric recorded in both field and laboratory settings (Fig. S6). There was no significant relationship between abalone size and P_{50} for either *H. sorenseni* or *H. rufescens* over the size range examined.

3.3. Temperature effects on metabolism and hypoxia tolerance

For the subset of *H. sorenseni* for which metabolic parameters were estimated at both 11 and 15°C, RMR was significantly higher at 15°C (n = 10, paired t test, t = -3.63, df = 9, P = 0.005) resulting in a Q_{10} of 2.89 ± 1.74 (Table 2). However, α and MMR were not significantly different in *H. sorenseni* between 11°C and 15°C (paired t test; t = -0.86, df = 9, P = 0.411; Table 2). This led to a significantly lower factorial aerobic scope for *H. sorenseni* at 15°C (paired t test; t = 3.01, df = 9, P = 0.015; Table 2). P_{90}, P_{75}, P_{50}, P_{25}, and P_{crit} values for *H. sorenseni* were higher at 15°C than at 11°C, but these differences were only significant for P_{25} (paired samples Wilcoxon test, V = 3, P = 0.010) and P_{crit} (paired samples Wilcoxon test; V = 5, P = 0.020; Table 2, Fig. S7A)

For *H. rufescens*, RMR was also significantly higher at 15°C than 11°C (n = 12, paired t test, t = -5.41, df = 11, P < 0.001) with a calculated Q_{10} of 2.24 ± 0.63 (Table 2). In contrast to *H. sorenseni*, α and MMR were both significantly elevated at 15°C (paired t test; t = -3.94, df = 11, P = 0.002; Table 2) while factorial aerobic scope was not significantly different between 11°C and 15°C (paired t test; t = 0.50, df = 11, P = 0.625; Table 2). For *H. rufescens*, there were also no significant differences in P_{90}, P_{75}, P_{50}, $P_{25,}$ and P_{crit} values between 11°C and 15°C (paired t test, df = 11, P > 0.05 for all comparisons; Table 2, Fig. S7B).

311 The calculated Q_{10} values between *H. sorenseni* and *H. rufescens* were not statistically
312 different (Wilcoxon test; $W = 59$, $P = 0.974$); however, *H. sorenseni* did have a higher standard
313 deviation for its Q_{10} value in comparison to *H. rufescens*.
314
315 **4. Discussion**
316 This study establishes valuable baseline metrics on the metabolism and hypoxia
317 sensitivity of the endangered white abalone in comparison to other abalone species. Specifically,
318 our results show that *H. sorenseni* has relatively low resting and maximum metabolic rates as
319 well as a low oxygen supply capacity (α) in comparison to *H. rufescens* and other abalone
320 species. This likely reflects its generally deep habitat where food may be less abundant and
321 energy likely needs to be conserved. In addition, *H. sorenseni* (and *H. rufescens*) oxygen
322 consumption rates generally show an atypical relationship with decreasing dissolved oxygen that
323 suggest some level of active metabolic depression that may allow for increased hypoxia
324 tolerance in comparison to some other abalone species that are less likely to regularly encounter
325 hypoxia. Here we discuss our results in the context of previous abalone research and ongoing
326 restoration efforts to help recover *H. sorenseni*.
327 The resting metabolic rate of *H. sorenseni* is one of the lowest of any abalone studied to
328 date, being significantly lower than that of *H. rufescens* and several other abalone species after
329 correction for temperature and body mass (Table 3). This lower metabolic demand is likely
330 functionally adaptive to the deeper depths typically inhabited by *H. sorenseni* (20-60 m),
331 particularly in areas outside the outer margins of kelp forests where they are largely reliant on
332 drift kelp settling down from shallower depths for food. The generally low metabolic demand of
333 *H. sorenseni* should thus allow for enhanced survival in less optimal habitat with scarcer food

availability. However, the intrinsically low metabolism of *H. sorenseni* will also likely contribute to comparatively slow growth rates, which could prolong captive growout and, ultimately, population recovery times.

In addition to a low metabolic rate, *H. sorenseni* shows an atypical relationship between oxygen consumption rate and environmental dissolved oxygen that is best represented as a logarithmic function (Fig. 3). This pattern suggests that *H. sorenseni* is partially conforming to ambient oxygen levels as metabolism decreases with progressive hypoxia. This rate of metabolic decline increases at lower oxygen levels until reaching a critical oxygen level (P_{crit}), at which point *H. sorenseni* appears to lose the ability to oxyregulate and becomes completely oxylimited. Prior to reaching the P_{crit}, our data suggest that both *H. sorenseni* (and *H. rufescens*) retain an aerobic scope that can be estimated by the aerobic supply capacity (Fig. 1, S2) as seen in high M_{O_2} outlier points in some of our individual respirometry trials (Fig S3). Retention of an aerobic scope with decreasing oxygen levels suggests that *H. sorenseni* and *H. rufescens* are actively lowering their metabolism. This would offer some protection against hypoxia exposure by limiting energetically expensive processes to times when dissolved oxygen is higher and not risking incursion of an oxygen debt that cannot be repaid under prolonged or increasingly severe hypoxia (Guppy and Withers, 1999, Seibel, 2011, Seibel *et al.*, 2014). It could also allow for emergency movements under hypoxia to either avoid predation or perhaps emerge from rocky crevices in search of better water flow and oxygen. This logarithmic-shaped pattern differs from that of most oxyregulating species, including most fishes, which typically display a broken stick relationship where the animal has a relatively stable oxygen consumption rate at oxygen levels above the P_{crit} (Farrell and Richards, 2009, Rogers *et al.*, 2016, Ultsch and Regan, 2019) as well as that of most oxyconforming species, which generally show a more linear or constant decrease

in M_{O_2} concomitant with decreasing oxygen and oxylimitation (Pörtner *et al*., 1985, Pörtner and Grieshaber, 1993). Abalone, and invertebrates in general, appear to express a wide range of metabolic and behavioral responses to hypoxia (Herreid II, 1980, Pörtner *et al*., 1985, Pörtner and Grieshaber, 1993, Grieshaber *et al.*, 1994, Riedel *et al.*, 2014, Galic *et al.*, 2019), and thus determining species-specific reactions to low oxygen is especially important. The logarithmic response to decreased dissolved oxygen in *H. sorenseni* and *H. rufescens* in this study may reflect their deeper and upwelling-prone habitat, in which they are more likely to regularly encounter episodic hypoxia and may thus actively lower their metabolic rate with decreasing environmental oxygen, while shallower-dwelling abalone species (which are less likely to encounter regular hypoxia) may attempt to maintain higher oxygen consumption rates until hitting a critical oxygen concentration at which point metabolic demands can no longer be maintained (Harris *et al*., 1999, Alter *et al.*, 2016, Chen *et al.*, 2020).

The shape of the metabolic response to decreasing environmental oxygen affects reported metrics of hypoxia tolerance (e.g., determination of P_{crit}) (Yeager and Ultsch, 1989, Marshall *et al.*, 2013, Claireaux and Chabot, 2016). Past studies on abalone metabolic responses to hypoxia have generally attempted to fit their data to the more commonly used broken-stick model in order to estimate a P_{crit} (Jan and Chang, 1983, Harris *et al.*, 1999, Taylor and Ragg, 2005), although our review of these datasets suggest that many may be more accurately described by a logarithmic relationship as observed here for *H. sorenseni* and *H. rufescens*. In this study, we used recent techniques by Seibel and colleagues (Seibel and Deutsch, 2020, Seibel *et al*., 2021) to quantify the oxygen supply capacity (α) which allows for determination of a P_{crit} despite a lack of a defined broken stick function and breakpoint (Fig. 1). We also quantified the effects of ambient oxygen level on metabolism by determining P_{90}, P_{75}, P_{50}, and P_{25} values, the dissolved

oxygen level when metabolic rate was 90%, 75%, 50%, and 25% of resting metabolic rate, which provide useful insight into how metabolism is affected by decreasing environmental oxygen. For example, while there were no observed significant differences in P_{90}, P_{75}, P_{50}, P_{25}, and P_{crit} between the *H. sorenseni* and *H. rufescens* at 15°C (Table 1, Fig. S5), the P_{50s} of *H. sorenseni* (26.7% air saturation) and *H. rufescens* (23.3%) were much lower than that of *H. laevigata* (68% at 18°C) (Harris *et al*., 1999). Thus, despite the immediate dampening of *H. sorenseni* and *H. rufescens* metabolic rate due to its logarithmic relationship with environmental oxygen, it appears that these species are both much more hypoxia tolerant than the shallower-dwelling *H. laevigata* at lower oxygen concentrations (e.g., the metabolic rate of *H. laevigata* was reduced to 50% at 68% air saturation, while that of *H. sorenseni* and *H. rufescens* was not reduced to 50% until 23-27% saturation).

These species-specific metabolic responses to reductions in environmental oxygen provide critical insight into the effects of hypoxia on abalone health and fitness. For example, when held under varying levels of hypoxia, *H. laevigata* showed reductions in food consumption, growth rates, and survival rates that mirrored its metabolic relationship with dissolved oxygen (Harris *et al.*, 1999). This indicates that mild reductions in dissolved oxygen are less likely to have significant impacts on more hypoxia tolerant species such as *H. sorenseni* and *H. rufescens*. However, despite the apparent enhanced hypoxia tolerance of *H. sorenseni* and *H. rufescens* in comparison to species like *H. laevigata*, exposure to lower oxygen levels is still likely to have both sublethal and potentially lethal effects. While the baseline metabolic data determined herein can thus inform comparative measures of hypoxia sensitivity for *H. sorenseni*, additional long-term growout studies under reduced oxygen levels would provide added quantifiable

insights into the effects of hypoxia on *H. sorenseni* survival, growth, feeding, behavior, and reproduction.

The negative effects of hypoxia on abalone can be further compounded by other environmental variables such as temperature (Tripp-Valdez *et al.*, 2017, Calderón-Liévanos *et al.*, 2021). Indeed, the cumulative stress of low oxygen and high temperatures is of particular concern in abalone aquaculture in which marine heat waves and environmental warming can have deleterious effects on densely packed and hypoxia-prone abalone farms in coastal surface waters (Nam *et al*., 2020, Shen *et al*., 2020, Shen *et al.*, 2021, Shen *et al*., 2022). Likewise, our results show that *H. sorenseni* metabolism is fairly sensitive to changes in temperature (Q_{10}=2.89), which appears to lead to decreased hypoxia tolerance at warmer temperatures as represented by increasing trends in P_{90}, P_{75}, P_{50}, P_{25}, and P_{crit} values and a decreased factorial aerobic scope with a change in temperature from 11°C to 15°C. While *H. sorenseni* live at deeper depths that are somewhat insulated from more extreme temperature fluctuations seen in surface-oriented coastal abalone farms, our results highlight the potential temporal, regional, and climatic impacts of the simultaneous shoaling of the oxygen minimum zone and an increase in coastal water temperatures (Grantham *et al*., 2004, Bograd *et al.*, 2008, Low *et al.*, 2021).

Although *H. sorenseni* and *H. rufescens* were shown to have similar mean P_{90}, P_{75}, P_{50}, P_{25}, and P_{crit} values, *H. sorenseni* generally exhibited a larger range in individual values compared to *H. rufescens* (Fig. S5). Such variation in hypoxia tolerance for *H. sorenseni* appears associated with the different shaped oxygen-sensitivity curves for some individuals, with 5 of 29 *H. sorenseni* showing a linear relationship (likely indicating increased oxyconformation and oxylimitation) that resulted in higher (less hypoxia-tolerant) P_{90}, P_{75}, P_{50}, P_{25} values and a lower oxygen supply capacity, MMR, and aerobic scope in comparison to those displaying the more

typically-observed logarithmic curves. Such differences in the shape of the relationship between oxygen consumption and dissolved oxygen level have been observed previously in abalone and other invertebrates and have often been attributed to differences in animal size or physiological state (e.g., fasted vs. unfasted) (Bayne, 1971, Gaty and Wilson, 1986). However, as all animals in the present study were in the same physiological state (all were fasted for 48 h) and there did not appear to be correlation of the shape of the relationship (log vs linear) with body size, we hypothesize that these differences likely indicate health and or fitness differences between individuals and possibly cohorts. Indeed, three out of the four highest P_{50} values determined came from abalone in the same cohort (*H. sorenseni* used in this experiment came from three cohorts spawned in 2014, 2016, and 2019; Fig. S8). This finding thus highlights the potential ramifications for fitness differences (i.e., reduced hypoxia tolerance, slower growth rates, etc.) in captive-bred *H. sorenseni* individuals or cohorts. In aquaculture optimization experiments, collection of *H. rufescens* from different areas along the California coast exposed to variable amounts of upwelling has shown inherent differences in tolerance to ocean acidification, highlighting natural variability and population level differences to regional environmental stressors (Swezey *et al.*, 2020). For the critically-endangered *H. sorenseni*, with limited broodstock within the White Abalone Recovery Consortium captive breeding program, the genetic diversity of captive spawned animals is a serious challenge that requires consideration of the phenotypic expression of tolerance to hypoxia, temperature, and other environmental factors to enhance potential outplanting success and ultimate recovery of the species in the wild. Only limited work on the genetic diversity of *H. sorenseni* has been conducted to date (Gruenthal and Burton, 2005, Masonbrink *et al.*, 2019), and expanded analysis to quantify the genetic diversity

447 of captive broodstock and offspring and its potential contribution to phenotypic variability in
448 tolerance to environmental stressors is needed.

449 As a main goal of the White Abalone Recovery Consortium is to rear *H. sorenseni* for
450 successful outplanting into the wild, we were particularly interested in examining the extent to
451 which abalone size may impact hypoxia sensitivity in order to determine if there is a potential
452 minimum size threshold for outplanting (for many marine species smaller individuals are more
453 sensitive to adverse environmental conditions, including hypoxia) (Nilsson and Östlund-Nilsson,
454 2008, Rogers *et al*., 2016, Verberk *et al.*, 2022). The relatively large size range examined here
455 (4.6 – 103.3 g, 34.8 – 91.5 mm shell length) showed that P_{50} did not change with body size (Fig.
456 S6) indicating that smaller abalone within this size range are just as tolerant to hypoxia exposure
457 as larger individuals. Currently, the White Abalone Recovery Consortium uses 25 mm shell
458 length as the minimum size threshold for outplanting *H. sorenseni* into the wild. Thus, while
459 additional respirometry studies are warranted on smaller individuals beyond the range studied
460 here, our results indicate that this minimum size threshold for outplanting is likely appropriate in
461 terms of hypoxia tolerance. In fact, recent work has shown that in some abalone species smaller-
462 sized animals may actually be more tolerant to hypoxia than older individuals (Vosloo *et al.*,
463 2013, Aalto *et al.*, 2020). For example, in the South African abalone (*H. midae*), smaller
464 juvenile abalone (mean shell length 41 mm) had higher anti-oxidant enzyme levels (associated
465 with minimizing DNA and protein damage caused by hypoxia and other stressors) than larger
466 adults (mean shell length 65 mm) (Vosloo *et al*., 2013). This is thought to be associated with the
467 variable oxygen levels encountered by small abalone within the diatom films upon which they
468 feed (Vosloo *et al*., 2013). Likewise, in order to avoid predation, juvenile abalone typically
469 spend more time within rocky and other substrate crevices that are more likely to experience

localized hypoxia associated with the respiration of other biota and more limited water circulation. While there does not appear to be a size effect on sensitivity to hypoxia, modeling for *H. sorenseni* outplanting, as well as population monitoring for *H. rufescens*, has revealed better stocking success occurs using larger individuals due to their higher survival rates (i.e., lower vulnerability to predation) and more immediate reproductive potential (Rogers-Bennett and Leaf, 2006, Leaf *et al.*, 2007, Li and Rogers-Bennett, 2017, Hofmeister *et al.*, 2018). Additionally, while some metabolic measurements have been determined for larval *H. sorenseni* (Moran and Manahan, 2003), there is little information about *H. sorenseni* larval hypoxia tolerance. Such information would be useful to help predict the effects of larval viability and dispersal under varying environmental conditions as outplanted individuals need to successfully reproduce in the wild.

5. Conclusions and Implications for Management

This study establishes valuable physiological metrics on the bioenergetics and hypoxia tolerance of *H. sorenseni* and *H. rufescens*. Importantly, we found that *H. sorenseni* have low resting metabolic rates likely reflective of their relatively deep habitat. This lower metabolism likely contributes to slower growth rates and has potential implications for population recovery times, both in terms of captive growout and the maturation and successful spawning of outplanted individuals. We also showed that *H. sorenseni* and *H. rufescens* show immediate reductions in their metabolism when exposed to lowering environmental oxygen levels. While this appears to be an active response to cope with hypoxic conditions, it could potentially have quantifiable effects on various aerobic processes including growth and reproductive output. Thus, outplant sites with higher dissolved oxygen levels would likely benefit *H. sorenseni*

493 metabolic-dependent processes. Current *H. sorenseni* outplanting sites in southern California
494 show mean dissolved oxygen levels ranging from 65-80% saturation (NOAA, unpublished data),
495 which indicates *H. sorenseni* resting metabolism is likely reduced by 9-15% under typical
496 conditions, although short bouts of lower dissolved oxygen levels down to 25-30% saturation
497 may periodically reduce abalone metabolism by up to 50% (Fig. S9).

498 Our work also revealed that *H. sorenseni* hypoxia tolerance did not differ significantly
499 with body size. However, certain *H. sorenseni* individuals did appear to have a lower aerobic
500 scope and to be less hypoxia tolerant than others, which provides important insight into natural
501 variation in intraspecific abalone environmental tolerance. We also found that increased
502 temperature resulted in decreased hypoxia tolerance for *H. sorenseni*, revealing the potential
503 compounding effects of low oxygen with other environmental factors. We thus encourage future
504 work to explore the variability in hypoxia tolerance and its interactions with compounding
505 factors such as temperature and pH. Finally, our study only examined the acute metabolic
506 response of *H. sorenseni* to hypoxia. Long-term exposure and growout experiments on *H.*
507 *sorenseni* would help us understand more chronic effects of low dissolved oxygen (which
508 juveniles may encounter within rocky crevices when outplanted) on *H. sorenseni* metabolism,
509 growth, and hypoxia tolerance, and contribute to optimizing best rearing and outplanting
510 practices.

511

512 **Acknowledgments**

513 The authors thank the Cultured Abalone Farm (Goleta, CA), Abalone Farm (Cayucos, CA) and
514 partners within the White Abalone Recovery Consortium for the abalone used in this study. The
515 authors also thank Kathy Swiney, Garrett Seibert, and Zach Skelton for help in abalone care and

husbandry, Sue Lowery and Kathy Swiney for reviewing drafts of this manuscript, and Tanya Prinzing for help with data analysis and R script. The authors also thank the peer reviewers of this manuscript, who helped strengthen the interpretation of results.

Funding

This research was supported by the NOAA Fisheries Office of Aquaculture.

Table 1: Metabolic and hypoxia sensitivity parameters (means ± standard deviation) estimated for 29 white (*H. sorenseni*) and 29 red (*H. rufescens*) abalone at 15°C.

Species	Mass (g)	Length (mm)	RMR ($mgO_2\ h^{-1}$)	α ($mgO_2\ h^{-1}\ \%O_2^{-1}$)	MMR ($mgO_2\ h^{-1}$)	FAS	P_{90}	P_{75}	P_{50}	P_{25}	P_{crit}
White abalone (*H. sorenseni*)	4.6 – 103.3	34.8 – 91.5	0.928* ± 0.186	0.0213* ± 0.0060	2.131* ± 0.599	2.38 ± 0.80	76.3 ± 7.1	51.4 ± 12.0	26.7 ± 11.6	12.9 ± 6.6	14.4 ± 6.3
Red abalone (*H. rufescens*)	7.7 – 103.3	39.1 – 94.0	1.483* ± 0.218	0.0352* ± 0.0075	3.517* ± 0.753	2.37 ± 0.37	74.6 ± 2.2	48.2 ± 3.5	23.3 ± 3.3	11.3 ± 2.3	15.2 ± 3.8

*Indicates significant difference between species. Abbreviations: Resting metabolic rate (RMR), α (oxygen supply capacity), MMR (maximum metabolic rate), FAS (factorial aerobic scope). For direct comparison between species, RMR, α, and MMR were scaled for each individual to a common mass of 40g using the scaling equations determined in Fig. 2.

559 **Table 2:** Effect of temperature (11 vs. 15°C) on metabolic and hypoxia sensitivity parameters
560 (means ± standard deviation) estimated for 10 white (*H. sorenseni*) and 12 red (*H. rufescens*)
561 abalone.

Species	Temp (°C)	Mass (g)	Length (mm)	RMR ($mgO_2\ h^{-1}$)	α ($mgO_2\ h^{-1}\ \%O_2^{-1}$)	MMR ($mgO_2\ h^{-1}$)	FAS	P_{90}	P_{75}	P_{50}	P_{25}	P_{crit}
White abalone	11	38.0 ± 7.1	66.0 ± 3.7	0.649* ± 0.116	0.0189 ± 0.0042	1.895 ± 0.419	2.93* ± 0.43	73.9 ± 5.1	47.1 ± 8.2	21.9 ± 6.5	9.0* ± 1.3	10.87* ± 2.22
(*H. sorenseni*)	15	31.9 ± 5.3	62.1 ± 3.5	0.934* ± 0.184	0.0206 ± 0.0048	2.055 ± 0.476	2.25* ± 0.57	76.8 ± 5.2	51.8 ± 9.0	27.0 ± 9.1	13.5* ± 5.2	17.77* ± 7.76
Red abalone	11	28.4 ± 3.8	60.8 ± 2.8	1.147* ± 0.151	0.0299* ± 0.0049	2.991* ± 0.490	2.62 ± 0.42	73.4 ± 2.0	46.2 ± 3.1	21.5 ± 2.9	10.0 ± 2.0	12.89 ± 3.31
(*H. rufescens*)	15	27.4 ± 3.5	59.9 ± 2.1	1.565* ± 0.176	0.0397* ± 0.0070	3.972* ± 0.701	2.54 ± 0.40	73.3 ± 2.5	46.0 ± 3.9	21.3 ± 3.6	9.9 ± 2.5	13.49 ± 4.01

562 *Indicates significant difference between temperature within a species. Abbreviations: Resting
563 metabolic rate (RMR), α (oxygen supply capacity), MMR (maximum metabolic rate), FAS
564 (factorial aerobic scope). For direct comparison, RMR, α, and MMR were scaled for each
565 individual to a common mass of 40g using the scaling equations determined in Fig. 2.

566 **Table 3**

567 Resting metabolic rates (RMR) of white (*H. sorenseni*) and red (*H. rufescens*) abalone in

568 comparison to other abalone species at 15 °C and scaled to a common body mass of 40.0 g.

Species	RMR ($mg\ O_2\ h^{-1}$)	Study
Small abalone (*H. diversicolor*)	0.860	Jan and Chang (1983)
Paua (*H. iris*)	0.865	Taylor and Ragg (2005)
White abalone (*H. sorenseni*)	0.928	Present study
South African abalone (*H. midae*)	0.976	Barkai and Griffiths (1987)
Ass's-ear abalone (*H. asinina*)	1.464	Baldwin *et al.* (2007)
Red abalone (*H. rufescens*)	1.482	Present study
Green abalone (*H. fulgens*)	1.747	Farías *et al.* (2003)
Pinto abalone (*H. kamtshatkana*)	1.755	Carefoot *et al.* (1993)
Green ormer (*H. tuberculata*)	2.022	Gaty and Wilson (1986)
South African abalone (*H. midae*)	2.048	Vosloo *et al*. (2013)
Pacific abalone (*H. discus hannai*)	2.173	Uki and Kikuchi (1975)
Pinto abalone (*H. kamtshatkana*)	2.509*	Paul and Paul (1998)
Greenlip abalone (*H. laevigata*)	3.870*	Harris *et al*. (1999)

569 For direct comparison with data from this study, resting metabolic rate for each species was

570 scaled to a common mass of 40.0 g using known species-specific scaling exponents (*H. discus*

571 *hannai*, $b = 0.8025$; *H. diverscolor*, $b = 0.6125$; *H. fulgens*, $b = 0.704$; H. *kamtshatkana, b* =

572 0.62; *H.* midae, $b = 0.78, 0.83$; *H. rufescens, b* = 0.7915; H. *sorenseni, b* = 0.9568; *H.*

573 *tuberculata*, $b = 0.869$) (Uki and Kikuchi, 1975, Jan and Chang, 1983, Gaty and Wilson, 1986,

574 Barkai and Griffiths, 1987, Carefoot *et al.*, 1993, Farías *et al.*, 2003, Vosloo *et al.*, 2013) or a
575 mass-scaling exponent of 0.80 if not previously determined. RMRs were also adjusted to a
576 common temperature of 15.0°C using species-specific metabolic temperature relationships (Uki
577 and Kikuchi, 1975, Gaty and Wilson, 1986, Barkai and Griffiths, 1987, Paul and Paul, 1998) or
578 using a Q_{10} of 2.0 if not previously determined. Note: Respirometry techniques differed between
579 studies, and some of the variation between species and conspecifics may reflect the different
580 methods. Trials in the present study were conducted with a one-hour acclimation period and
581 utilized plastic isolation disks to transfer the abalone into the respirometer to minimize any
582 metabolic signature associated with handling stress, while also minimizing the time for
583 introduced bacteria to establish and create a strong background respiration rate that could mask
584 the abalone oxygen consumption rate. *The much higher metabolic rates for *H. kamtshatkana*
585 (Paul and Paul, 1998) and *H. laevigata* (Harris *et al*., 1999) in comparison to the other species
586 may reflect the long acclimation times (3-4 days) for abalone in the respirometer, which may
587 have introduced a heavy bacterial load that could increase the measured oxygen consumption
588 rate.

589 **Figure Captions:**

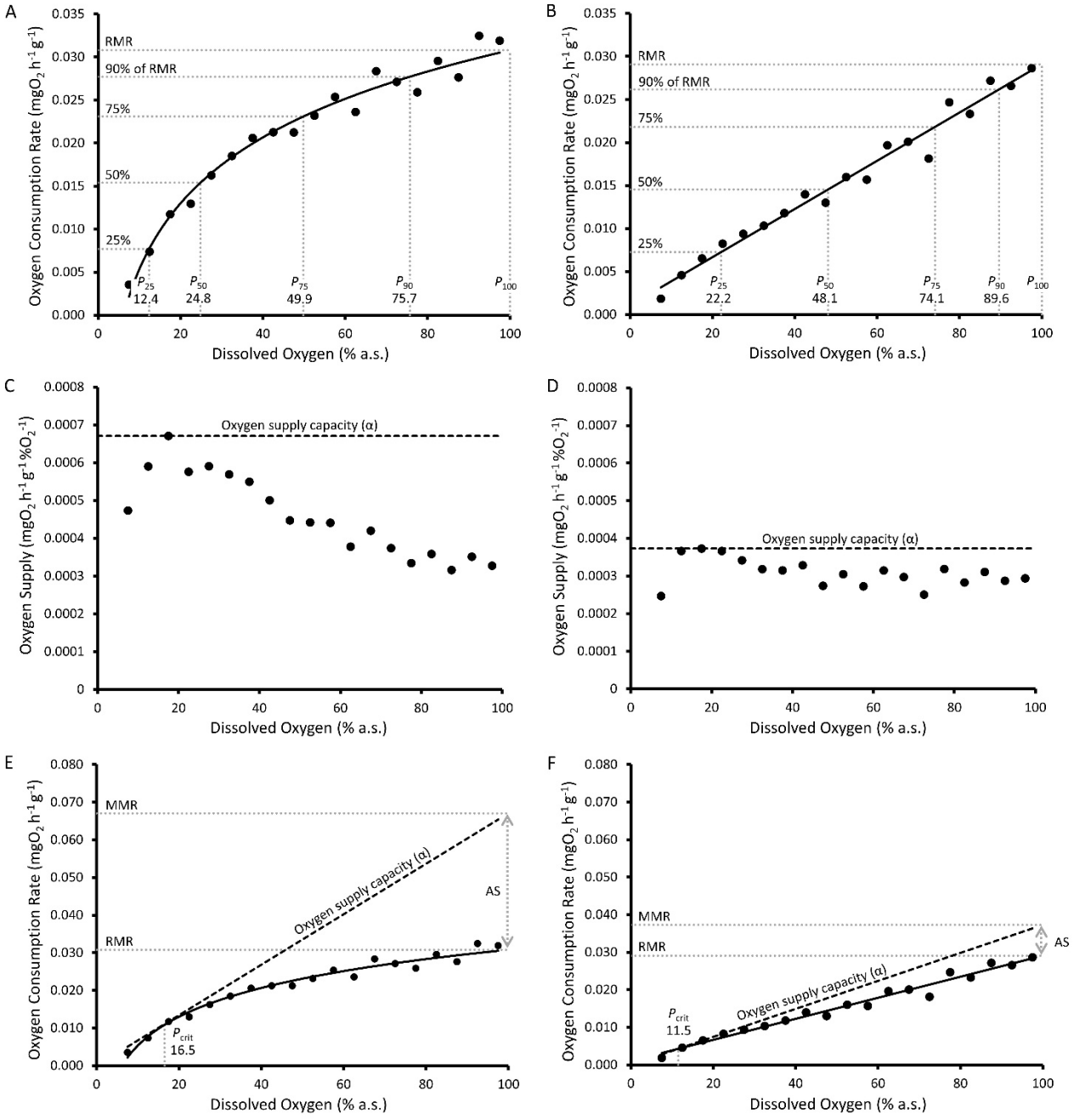

590

591 **Fig. 1.** Relationships between oxygen consumption rate ($mgO_2\ h^{-1}\ g^{-1}$) and environmental

592 dissolved oxygen level (% air saturation) at 15°C for white abalone (*H. sorenseni*). (A) A

593 logarithmic-shaped oxygen consumption profile from an 81.1 g and 82.7 mm white abalone. (B)

594 A linear-shaped oxygen consumption profile for a 14.6 g and 48.9 mm white abalone. These

curves were used to determine the P_{90}, P_{75}, P_{50}, and P_{25} (gray dotted lines) representing the environmental dissolved oxygen level at which the oxygen consumption of each individual was 90%, 75%, 50%, 25% of resting metabolic rate (RMR, as estimated by P_{100}). (C, D) Oxygen supply capacity for the 81.1 g white abalone in (A) and 14.6 g white abalone in (B) respectively, showing the change in oxygen consumption per available unit of environmental dissolved oxygen. (E, F) Combined oxygen consumption profiles with respective oxygen supply capacity for the 81.1 g white abalone from (A,C) and 14.6 g white abalone from (B,D) used to estimate the maximum metabolic rate (MMR), aerobic scope (AS), and P_{crit}.

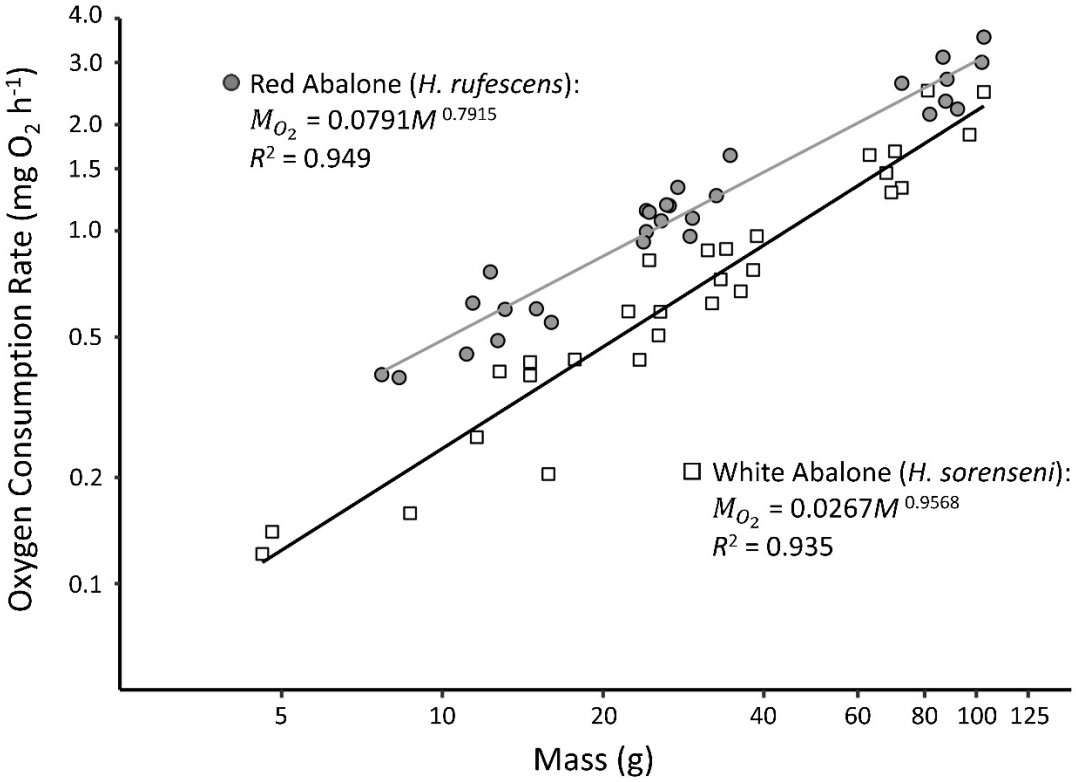

Fig. 2. The relationship of resting metabolic rate (mg O_2 h^{-1}) versus total body mass (g) for white (*H. sorenseni,* n = 29) and red abalone (*H. rufescens*, n = 29) at 15°C. Lines depict the best-fit allometric scaling equation for each species.

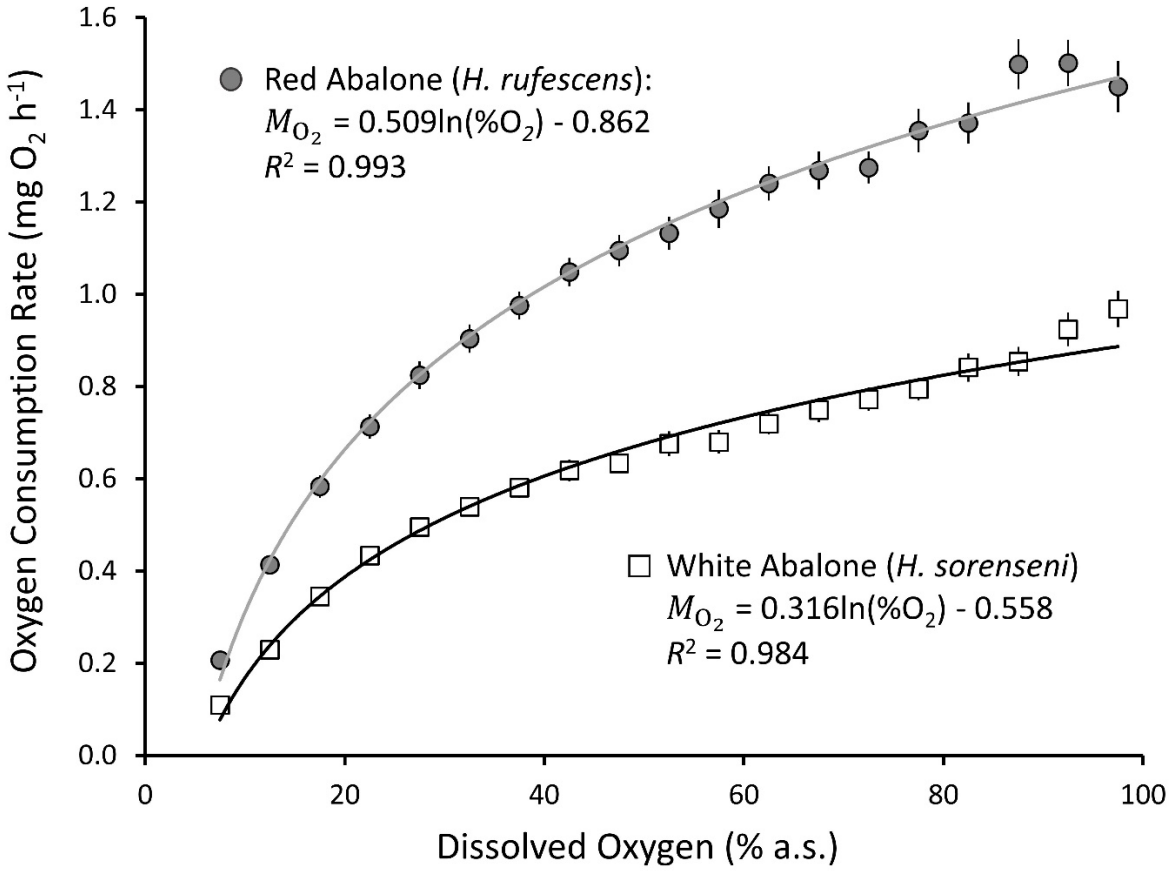

621

622

623 **Fig. 3.** Mean oxygen consumption rates (M_{O_2}) in relation to environmental dissolved oxygen (%
624 air saturation) for white (*H. sorenseni*, n = 29) and red abalone (*H. rufescens*, n = 29) at 15°C.
625 All *H. sorenseni* and *H. rufescens* individuals were scaled to a common total body mass of 40 g
626 (using a scaling exponent of 0.9568 for *H. sorenseni* and 0.7915 for *H. rufescens*, see Fig. 2) for
627 direct comparison between species.

628 **REFERENCES**

629

630 Aalto, E.A., Barry, J.P., Boch, C.A., Litvin, S.Y., Micheli, F., Woodson, C.B., De Leo, G.A.,
631 2020. Abalone populations are most sensitive to environmental stress effects on adult
632 individuals. *Mar. Ecol. Prog. Ser.* 643, 75-85.

633 Alter, K., Andrewartha, S.J., Elliott, N.G., 2016. Hatchery conditions do not negatively impact
634 respiratory response of early life-stage development in Australian hybrid abalone. *J. Shellfish*
635 *Res.* 35, 585-591.

636 Baldwin, J., Elias, J.P., Wells, R.M.G., Donovan, D.A., 2007. Energy metabolism in the tropical
637 abalone, *Haliotis asinina* Linné: Comparisons with temperate abalone species. *J. Exp. Mar. Biol.*
638 *Ecol.* 342, 213-225.

639 Barkai, R., Griffiths, C.L., 1987. Consumption, absorption efficiency, respiration and excretion
640 in the South African abalone *Haliotis midae*. *S. Afr. J. Mar. Sci.* 5, 523-529.

641 Bayne, B.L., 1971. Oxygen consumption by three species of lamellibranch mollusc in declining
642 ambient oxygen tension. *Comp. Biochem. Physiol.* 40A, 955-970.

643 Boch, C.A., Micheli, F., AlNajjar, M., Monismith, S.G., Beers, J.M., Bonilla, J.C., Espinoza,
644 A.M., Vazquez-Vera, L., Woodson, C.B., 2018. Local oceanographic variability influences the
645 performance of juvenile abalone under climate change. *Sci. Rep.* 8, 5501.

646 Bograd, S.J., Castro, C.G., Di Lorenzo, E., Palacios, D.M., Bailey, H., Gilly, W., Chavez, F.P.,
647 2008. Oxygen declines and the shoaling of the hypoxic boundary in the California Current.
648 *Geophys. Res. Lett.* 35, L12607.

649 Butler, J., Neuman, M., Pinkard, D., Kvitek, R., Cochrane, G., 2006. The use of multibeam sonar
650 mapping techniques to refine population estimates of the endangered white abalone (*Haliotis*
651 *sorenseni*). *Fish. Bull.* 104, 521-532.

652 Calderón-Liévanos, S., Hernández-Saavedra, N.Y., Lluch-Cota, S.E., Cruz-Hernández, P.,
653 Ascencio-Valle, F.D.J., Sicard, M.T., 2019. Survival and respiration of green abalone (*Haliotis*
654 *fulgens*) facing very short-term marine environmental extremes. *Mar. Freshw. Behav. Physiol.*
655 52, 1-15.

656 Calderón-Liévanos, S., Lluch-Cota, S.E., Hernández-Saavedra, N.Y., Racotta, I.S., Cruz-
657 Hernández, P., Ascencio, F., Sicard, M.T., 2021. Responses of the green abalone *Haliotis fulgens*
658 (Philippi, 1845) to sudden and recurring extreme environmental variations. *J. Shellfish Res.* 40,
659 127-136.

660 Carefoot, T.H., Qian, P.-Y., Taylor, B.E., West, T., Osborne, J., 1993. Effect of starvation on
661 energy reserves and metabolism in the Northern abalone, *Haliotis kamtschatkana*. *Aquaculture*
662 118, 315-325.

663 Catton, C.A., Stierhoff, K.L., Rogers-Bennett, L., 2016. Population status assessment and
664 restoration modeling of white abalone *Haliotis sorenseni* in California. *J. Shellfish Res.* 35, 593-
665 599.

666 Chabot, D., Steffensen, J.F., Farrell, A.P., 2016. The determination of standard metabolic rate in
667 fishes. *J. Fish Biol.* 88, 81-121.

668 Chen, N., Shen, Y., Yu, F., Luo, X., You, W., Ke, C., 2020. A new indicator of hypoxia
669 tolerance in abalone, developed based on heart rate fluctuations. *Aquaculture* 519, 734903.

670 Childress, J.J., Seibel, B.A., 1998. Life at stable low oxygen levels: Adaptations of animals to
671 oceanic oxygen minimum layers. *J. Exp. Biol.* 201, 1223-1232.

672 Claireaux, G., Chabot, D., 2016. Responses by fishes to environmental hypoxia: integration
673 through Fry's concept of aerobic metabolic scope. *J. Fish Biol.* 88, 232-251.

674 Davis, G.E., Haaker, P.L., Richards, D.V., 1996. Status and trends of white abalone at the
675 California Channel Islands. *Trans. Am. Fish. Soc.* 125, 42-48.

676 DiNardo, J., Stierhoff, K.L., Semmens, B.X., 2021. Modeling the past, present, and future
677 distributions of endangered white abalone (*Haliotis sorenseni*) to inform recovery efforts in
678 California. *PLOS ONE* 16, e0259716.

679 Farías, A., García-Esquivel, Z., Viana, M.T., 2003. Physiological energetics of the green
680 abalone, *Haliotis fulgens*, fed on a balanced diet. *J. Exp. Mar. Biol. Ecol.* 289, 263-276.

681 Farrell, A.P., Richards, J.G., 2009. Defining hypoxia: An integrative synthesis of the responses
682 of fish to hypoxia. In: Richards, J.G., Farrell, A.P., Brauner, C.J. (Eds.), Fish Physiology Vol. 27:
683 Hypoxia, Academic Press, Amsterdam, pp 487-503.

684 Frank, L.N., Stuart, K., Skelton, Z., Drawbridge, M., Hyde, J.R., Lowery, M.S., Wegner, N.C.,
685 2021. Exercise duration and cohort affect variability and longevity of the response to exercise
686 training in California Yellowtail (*Seriola dorsalis*). *Aquaculture* 540, 736684.

687 Frieder, C.A., Nam, S.H., Martz, T.R., Levin, L.A., 2012. High temporal and spatial variability
688 of dissolved oxygen and pH in a nearshore California kelp forest. *Biogeosciences* 9, 3917-3930.

689 Galic, N., Hawkins, T., Forbes, V.E., 2019. Adverse impacts of hypoxia on aquatic invertebrates:
690 A meta-analysis. *Sci. Total Environ.* 652, 736-743.

691 Gaty, G., Wilson, J., 1986. Effect of body size, starvation, temperature and oxygen tension on the
692 oxygen consumption of hatchery-reared ormers *Haliotis tuberculata* L. *Aquaculture* 56, 229-237.

693 Grantham, B.A., Chan, F., Nielsen, K.J., Fox, D.S., Barth, J.A., Huyer, A., Lubchenco, J.,
694 Menge, B.A., 2004. Upwelling-driven nearshore hypoxia signals ecosystem and oceanographic
695 changes in the northeast Pacific. *Nature* 429, 749-754.

696 Grieshaber, M.K., Hardewig, I., Kreutzer, U., Pörtner, H.-O., 1994. Physiological and metabolic
697 responses to hypoxia in invertebrates. *Rev. Physiol. Biochem. Pharmacol.* 125, 43-147.

698 Gruenthal, K.M., Burton, R.S., 2005. Genetic diversity and species identification in the
699 endangered white abalone (*Haliotis sorenseni*). *Conserv. Genet.* 6, 929-939.

700 Guppy, M., Withers, P., 1999. Metabolic depression in animals, physiological perspectives and
701 biochemical generalizations. *Biol. Rev.* 74, 1-40.

702 Harris, J.O., Maguire, G.B., Edwards, S.J., Johns, D.R., 1999. Low dissolved oxygen reduces
703 growth rate and oxygen consumption rate of juvenile greenlip abalone, *Haliotis laevigata*
704 Donovan. *Aquaculture* 174, 265-278.

705 Herreid II, C.F., 1980. Hypoxia in invertebrates. *Comp. Biochem. Physiol.* 67A, 311-320.

706 Hobday, A.J., Tegner, M.J., Haaker, P.L., 2001. Over-exploitation of a broadcast spawning
707 marine invertebrate: Decline of the white abalone. *Rev. Fish Biol. Fish.* 10, 493-514.

Hofmeister, J.K.K., Kawana, S.K., Walker, B.J., Catton, C.A., Taniguchi, I., Stein, D.M., Sowul, K., Rogers-Bennett, L., 2018. Temporal and spatial patterns in behavioral responses of marine predators to a sudden influx of abalone prey (*Haliotis rufescens*). *Hydrobiologia* 813, 123-136.

Jan, R.-Q., Chang, K.-H., 1983. The oxygen consumption by Formosan abalone, *Haliotis diversicolor supertexta* Lischke, during decline of ambient oxygen. *Bull. Inst. Zool., Academia Sinica* 22, 43-48.

Karpov, K.P., Haaker, P.L., Taniguchi, I.K., Rogers-Bennett, L., 2000. Serial depletion and the collapse of the California abalone (*Haliotis* spp.) fishery. In: Campbell, A. (Ed.), Workshop on Rebuilding Abalone Stocks in British Columbia Vol. 130, Canadian Special Publication of Fisheries and Aquatic Sciences, Ottawa, Canada, pp 11-24.

Kekuewa, S.A.H., Courtney, T.A., Cyronak, T., Andersson, A.J., 2022. Seasonal nearshore ocean acidification and deoxygenation in the Southern California Bight. *Sci. Rep.* 12, 17969.

Kim, T.W., Barry, J.P., Micheli, F., 2013. The effects of intermittent exposure to low-pH and low-oxygen conditions on survival and growth of juvenile red abalone. *Biogeosciences* 10, 7255-7262.

Leaf, R.T., Rogers-Bennett, L., Haaker, P.L., 2007. Spatial, temporal, and size-specific variation in mortality estimates of red abalone, *Haliotis rufescens*, from mark-recapture data in California. *Fish. Res.* 83, 341-350.

Li, Y., Rogers-Bennett, L. 2017. Evaluating factors affecting restoration of an endangered marine broadcast-spawning invertebrate using an individual-based model of white abalone. *Endanger. Species Res.* 32, 293-308.

729 Low, N.H.N., Micheli, F., Aguilar, J.D., Arce, D.R., Boch, C.A., Bonilla, J.C., Bracamontes,
730 M.Á., De Leo, G., Diaz, E., Enríquez, E., *et al.* 2021. Variable coastal hypoxia exposure and
731 drivers across the southern California Current. *Sci. Rep.* 11, 10929.

732 Marshall, D.J., Bode, M., White, C.R., 2013. Estimating physiological tolerances – a comparison
733 of traditional approaches to nonlinear regression techniques. *J. Exp. Biol.* 216, 2176-2182.

734 Masonbrink, R.E., Purcell, C.M., Boles, S.E., Whitehead, A., Hyde, J.R., Seetharam, A.S.,
735 Severin, A.J., 2019. An annotated genome for *Haliotis rufescens* (red abalone) and resequenced
736 green, pink, pinto, black, and white abalone species. *Genome Biol. Evol.* 11, 431-438.

737 Moran, A.L., Manahan, D.T., 2003. Energy metabolism during larval development of green and
738 white abalone, *Haliotis fulgens* and *H. sorenseni*. *Biol. Bull.* 204, 270-277.

739 Morash, A.J., Alter, K., 2016. Effects of environmental and farm stress on abalone physiology:
740 perspectives for abalone aquaculture in the face of global climate change. *Rev. Aquac.* 8, 342-
741 368.

742 Nam, S.-E., Haque, M.N., Lee, J.S., Park, H.S., Rhee, J.-S., 2020. Prolonged exposure to
743 hypoxia inhibits the growth of Pacific abalone by modulating innate immunity and oxidative
744 status. *Aquat. Toxicol.* 227, 105596.

745 Nilsson, G.E., Östlund-Nilsson, S., 2008. Does size matter for hypoxia tolerance in fish? *Biol.*
746 *Rev.* 83, 173-189.

747 NMFS, 2008. White Abalone Recovery Plan (*Haliotis sorenseni*). National Marine Fisheries
748 Service, Long Beach, CA.

749 Parnell, P.E., Levin, L.A., Navarro, M.O., 2020. Gauging oxygen risk and tolerance for the
750 megafauna of the Southern California shelf based on in situ observation, species mobility, and
751 seascape. *ICES J. Mar. Sci.* 77, 1941-1952.

752 Paul, A.J., Paul, J.M., 1998. Respiration rate and thermal tolerances of pinto abalone *Haliotis*
753 *kamtschatkana*. *J. Shellfish Res.* 17, 743-746.

754 Pörtner, H.-O., Heisler, N., Grieshaber, M., 1985. Oxygen consumption and mode of energy
755 production in the intertidal worm *Sipunculus nudus* L.: Definition and characterization of the
756 critical P_{O_2} for an oxyconformer. *Resp. Physiol.* 59, 361-377.

757 Pörtner, H.-O., Grieshaber, M.K., 1993. Critical P_{O_2}(s) in oxyconforming and oxyregulating
758 animals: Gas exchange, metabolic rate and the mode of energy production. In: Bicudo, J.E.P.W.
759 (Ed.), The Vertebrate Gas Transport Cascade: Adaptations to Environment and Mode of Life,
760 CRC Press, Boca Raton, pp 330-357.

761 R Core Team (2024) R: A language and environment for statistical computing. R Foundation for
762 Statistical Computing, Vienna, Austria. https://www.R-project.org/.

763 Reemeyer, J.E., Rees, B.B., 2019. Standardizing the determination and interpretation of P_{crit} in
764 fishes. *J. Exp. Biol.* 222, jeb210633.

765 Riedel, B., Pados, T., Pretterebner, K., Schiemer, L., Steckbauer, A., Haselmair, A., Zuschin, M.,
766 Stachowitsch, M., 2014. Effect of hypoxia and anoxia on invertebrate behaviour: ecological
767 perspectives from species to community level. *Biogeosciences* 11, 1491-1518.

768 Rogers-Bennett, L., Aquilino, K.M., Catton, C.A., Kawana, S.K., Walker, B.J., Ashlock, L.W.,
769 Marshman, B.C., Moore, J.D., Taniguchi, I.K., Gilardi, K.V., *et al.,* 2016. Implementing a
770 restoration program for the endangered white abalone (*Haliotis sorenseni*) in California. *J.*
771 *Shellfish Res.* 35, 611-618.

772 Rogers-Bennett, L., Haaker, P.L., Huff, T.O., Dayton, P.K., 2002. Estimating baseline
773 abundances of abalone in California for restoration. *CalCOFI Rep.* 43, 97-111.

774 Rogers-Bennett, L., Leaf, R.T., 2006. Elasticity analyses of size-based red and white abalone
775 matrix models: Management and conservation. *Ecol. Appl.* 16, 213-224.

776 Rogers, N.J., Urbina, M.A., Reardon, E.E., McKenzie, D.J., Wilson, R.W., 2016. A new analysis
777 of hypoxia tolerance in fishes using a database of critical oxygen level (P_{crit}). *Conserv. Physiol.*
778 4, cow012.

779 Seibel, B.A., 2011. Critical oxygen levels and metabolic suppression in oceanic oxygen
780 minimum zones. *J. Exp. Biol.* 214, 326-336.

781 Seibel, B.A. and Deutsch, C. 2020. Oxygen supply capacity in animals evolves to meet
782 maximum demand at the current oxygen partial pressure regardless of size or temperature. *J.*
783 *Exp. Biol.* 224: jeb.210492.

784 Seibel, B.A., Andres, A., Birk, M.A., Burns, A.L., Shaw, C.T., Timpe, A.W., Welsh, C.J., 2021.
785 Oxygen supply capacity breathes new life into the critical oxygen partial pressure (P_{crit}). *J. Exp.*
786 *Biol*. 224: jeb242210.

787 Seibel, B.A., Häfker, N.S., Trübenbach, K., Zhang, J., Tessier, S.N., Pörtner, H.-O., Rosa, R.,
788 Storey. K.B., 2014. Metabolic suppression during protracted exposure to hypoxia in the jumbo
789 squid, *Dosidicus gigas*, living in an oxygen minimum zone. *J. Exp. Biol.* 217, 2555-2568.

790 Shen, Y., Gan, Y., Xiao, Q., Huang, Z., Liu, J., Gong, S., Wang, Y., Yu, W., Luo, X., Ke, C.,
791 You, W., 2022. Divergent carry-over effects of hypoxia during the early development of abalone.
792 *Environ. Sci. Technol.* 56, 17836-17848.

793 Shen, Y., Huang, M., You, W., Luo, X., Ke, C., 2020. The survival and respiration response of
794 two abalones under short-term hypoxia challenges. *Aquaculture* 529, 735658.

795 Shen, Y., Zhang, Y., Xiao, Q., Gan, Y., Wang, Y., Pang, G., Huang, Z., Yu, F., Luo, X., Ke, C.,
796 You, W., 2021. Distinct metabolic shifts occur during the transition between normoxia and
797 hypoxia in the hybrid and its maternal abalone. *Sci. Total Environ.* 794, 148698.

798 Stierhoff, K.L., Neuman, M., Butler, J.L., 2012. On the road to extinction? Population declines
799 of the endangered white abalone, *Haliotis sorenseni*. *Biol. Conserv.* 152, 46-52.

800 Stierhoff, K.L., Neuman, M., Mau, S.A., Murfin, D.W., 2014. White abalone at San Clemente
801 Island: Population estimates and management recommendations. NOAA Technical
802 Memorandum NMFS-SWFSC-527, US Department of Commerce, La Jolla, CA.

803 Swezey, D.S., Boles, S.E., Aquilino, K.M., Stott, H.K., Bush, D., Whitehead, A., Rogers-
804 Bennett, L., Hill, T.M., Sanford, E., 2020. Evolved differences in energy metabolism and growth
805 dictate the impacts of ocean acidification on abalone aquaculture. *Proc. Natl. Acad. Sci.* 117,
806 26513-26519.

807 Taylor, H., Ragg, N., 2005. The role of body surfaces and ventilation in gas exchange of the
808 abalone, *Haliotis iris*. *J. Comp. Physiol. B* 175, 463-478.

809 Tripp-Valdez, M.A., Bock, C., Lucassen, M., Lluch-Cota, S.E., Sicard. M.T., Lannig, G.,
810 Pörtner, H.O., 2017. Metabolic response and thermal tolerance of green abalone juveniles
811 (*Haliotis fulgens*: Gastropoda) under acute hypoxia and hypercapnia. *J. Exp. Mar. Biol. Ecol.*
812 497, 11-18.

813 Uki, N., Kikuchi, S., 1975. Oxygen consumption of the abalone, *Haliotis discus hannai* in
814 relation to body size and temperature. *Bull. Tohoku Reg. Fish. Res. Lab.* 35, 73-84.

815 Ultsch, G.R., Regan, M.D., 2019. The utility and determination of P_{crit} in fishes. *J. Exp. Biol.*
816 222, jeb203646.

817 Vaquer-Sunyer, R., Duarte, C.M., 2008. Thresholds of hypoxia for marine biodiversity. *Proc.*
818 *Natl. Acad. Sci.* 105, 15452-15457.

819 Verberk, W.C.E.P., Sandker, J.F., van de Pol, I.L.E., Urbina, M.A., Wilson, R.W., McKenzie,
820 D.J., Leiva, F.P., 2022. Body mass and cell size shape the tolerance of fishes to low oxygen in a
821 temperature-dependent manner. *Glob. Chang. Biol.* 28, 5695-5707.

822 Vosloo, A., Laas, A., Vosloo, D., 2013. Differential responses of juvenile and adult South
823 African abalone (*Haliotis midae* Linnaeus) to low and high oxygen levels. *Comp. Biochem.*
824 *Physiol.* 164A, 192-199.

825 Yeager, D.P., Ultsch, G.R., 1989. Physiological regulation and conformation: A BASIC program
826 for the determination of critical points. *Physiol. Zool.* 62, 888-907.

827 **Supplementary Materials Figures:**

828

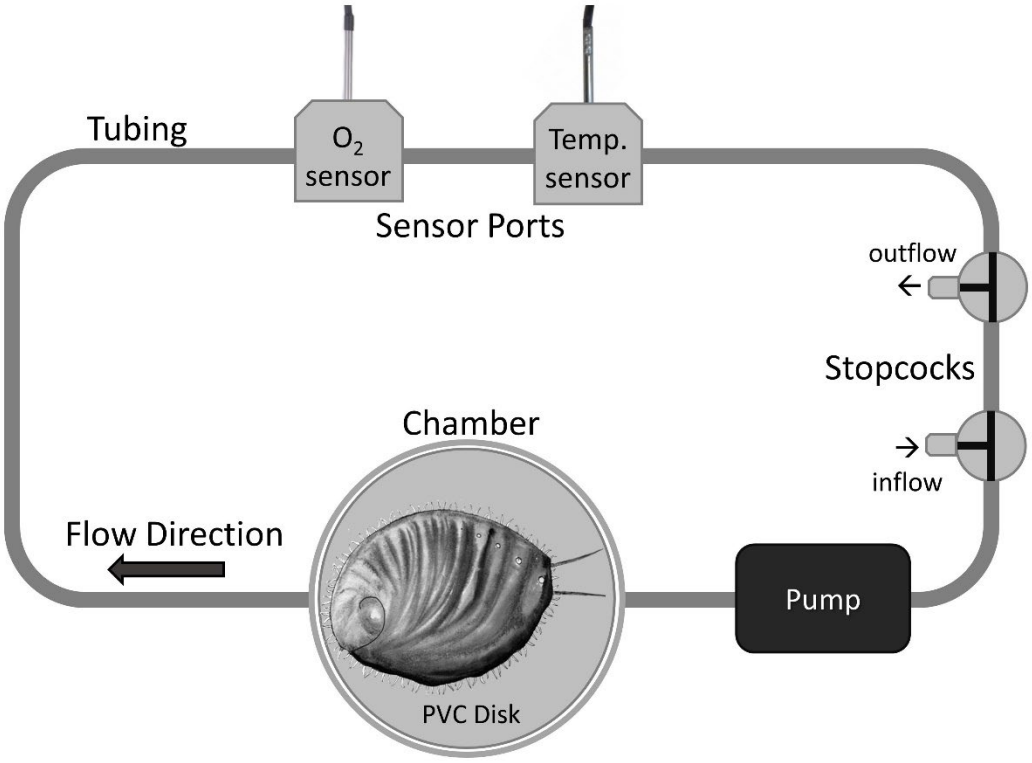

829

830 **Fig. S1.** Schematic of the abalone respirometry system composed of an acrylic cylindrical
831 holding chamber and a recirculating loop for monitoring dissolved oxygen concentration and
832 temperature. Three-way stopcocks within the loop were used to manually open and close the
833 system to the surrounding buffer tank seawater kept at a constant targeted temperature of 11.0 or
834 15.0°C. Prior to a respirometry trial the abalone was placed on a PVC disk cutout that was used
835 to transfer the animal from an isolated holding chamber into the respirometer in order to
836 minimize handling stress and air exposure.
837
838
839

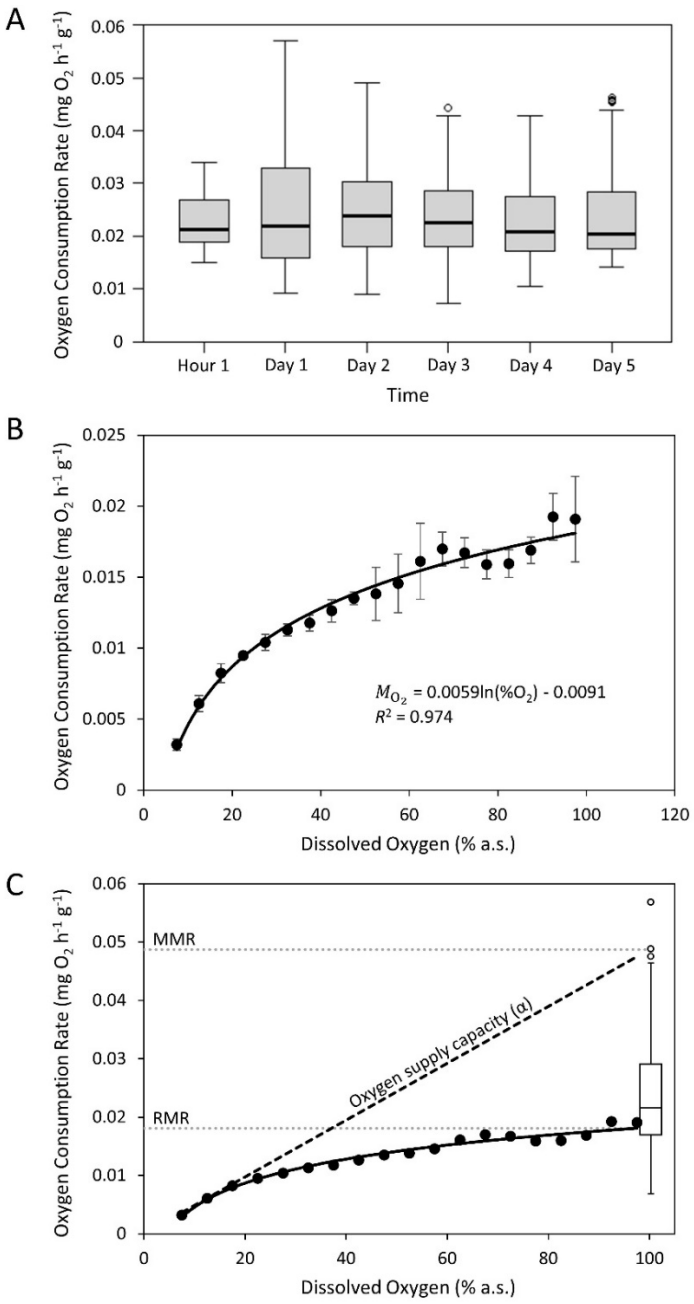

Fig. S2. Supplementary respirometry trials for three red abalone (*H. rufescens*) at 15°C showing: (A) Little change in mean oxygen consumption rate (mg O_2 h^{-1} g^{-1}) over five days in the respirometer. (B) Mean oxygen consumption rate (± SE) in response to declining dissolved oxygen (% air saturation) following five days in the respirometer. (C) Combined plot of (A) and (B) showing mean abalone oxygen consumption in response to declining dissolved oxygen in comparison to that measured over five days in the respirometer (box plot). The oxygen supply capacity (α, dashed line) calculated as a function of declining oxygen was used to estimate maximum metabolic rate (MMR), which closely matches maximum oxygen consumption measured over five days in the respirometer. Resting metabolic rate (RMR) was estimated from the logarithmic relationship of oxygen consumption at 100% a.s., which closely matches the $q_{0.25}$ of the oxygen consumption rates measured over five days. For all plots, individual abalone oxygen consumption data were scaled to a common body mass of 40 g using b = 0.7915.

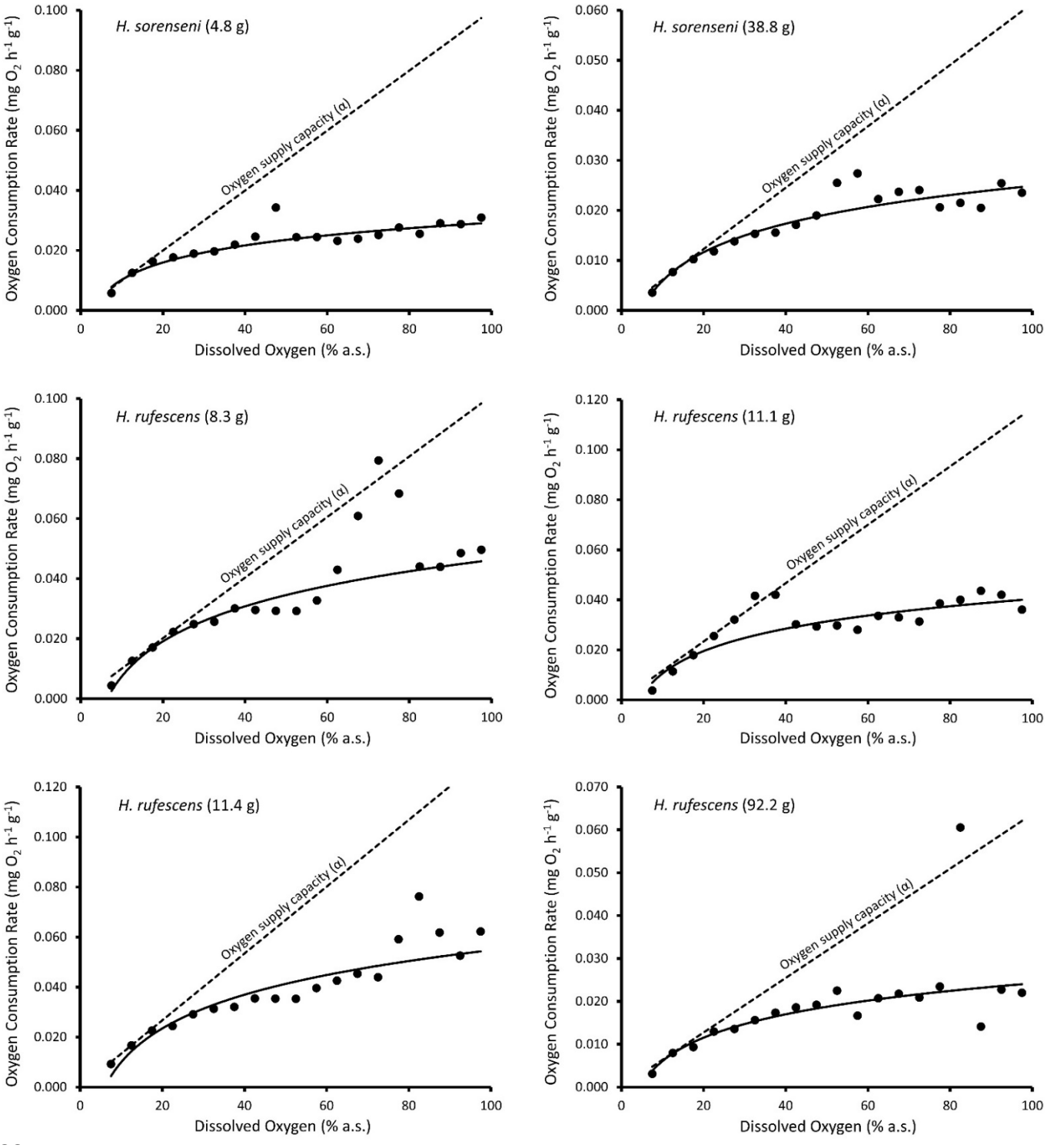

Fig. S3. Relationships of oxygen consumption rate (mg O_2 h^{-1} g^{-1}) and environmental dissolved oxygen (% air saturation) (solid black line) at 15°C for six white (*H. sorenseni*) and red abalone (*H. rufescens*) individuals showing the estimated oxygen supply capacity (α, dashed line) in relation to occasional high outlier points likely associated with abalone activity within the respirometer.

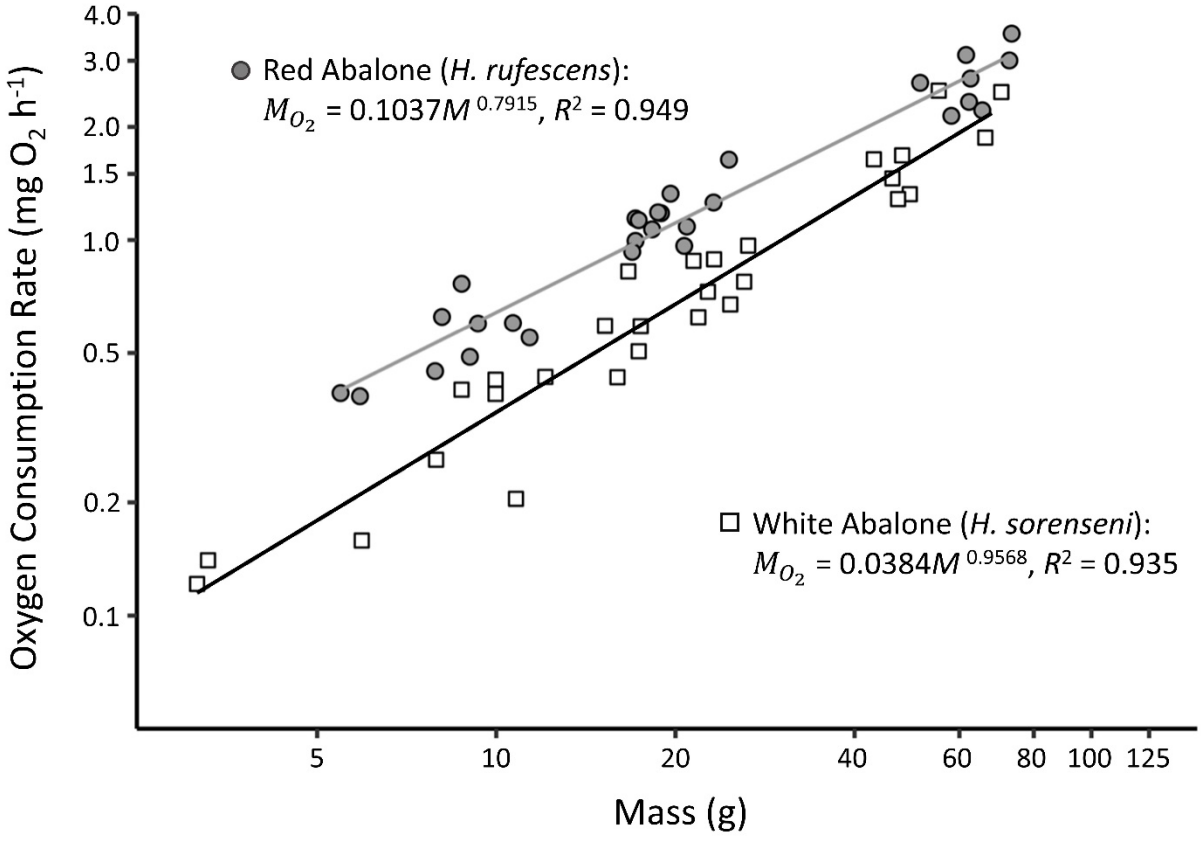

Fig. S4. The relationship of resting metabolic rate (mg O_2 h^{-1}) versus live tissue mass (total mass – shell mass, g) for white (*H. sorenseni,* n = 29) and red abalone (*H. rufescens*, n = 29) at 15°C. Lines depict the best-fit allometric scaling equation for each species.

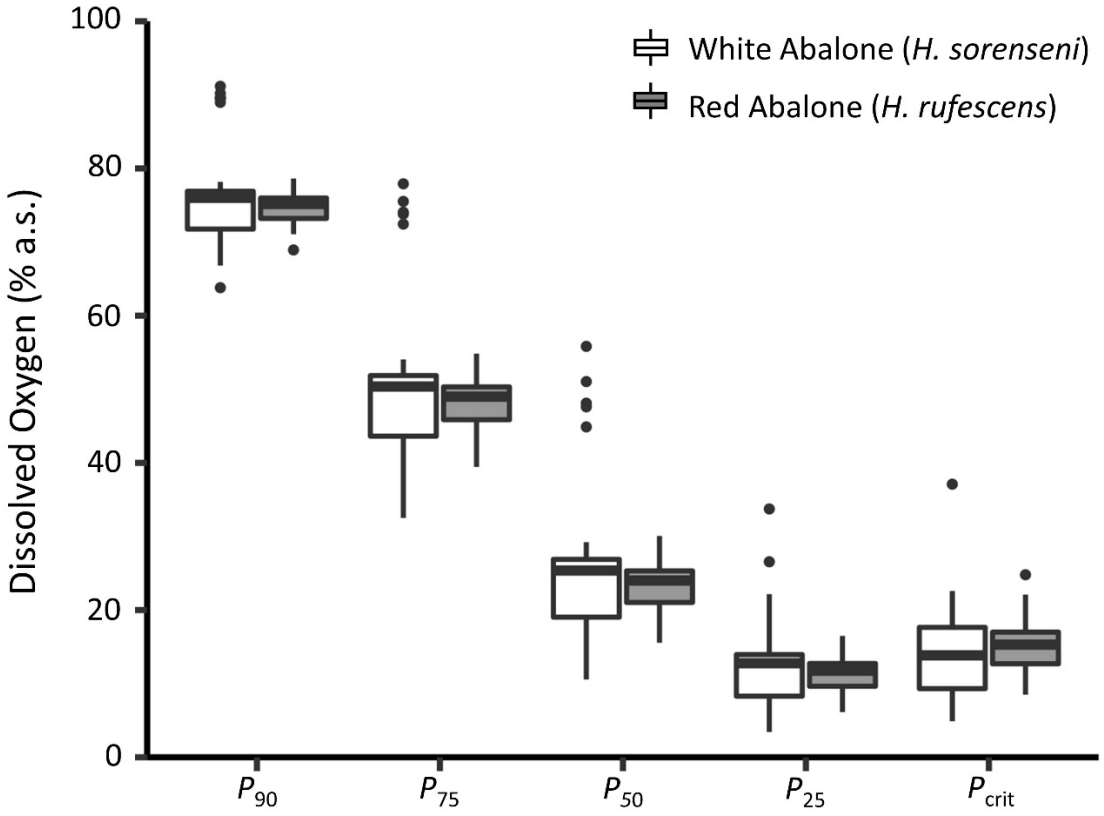

Fig. S5. Boxplots showing the hypoxia tolerance measures of P_{90}, P_{75}, P_{50}, P_{25}, and P_{crit} (dissolved oxygen level in percent air saturation) for white (*H. sorenseni*, n = 29) and red abalone (*H. rufescens*, n = 29) at 15°C.

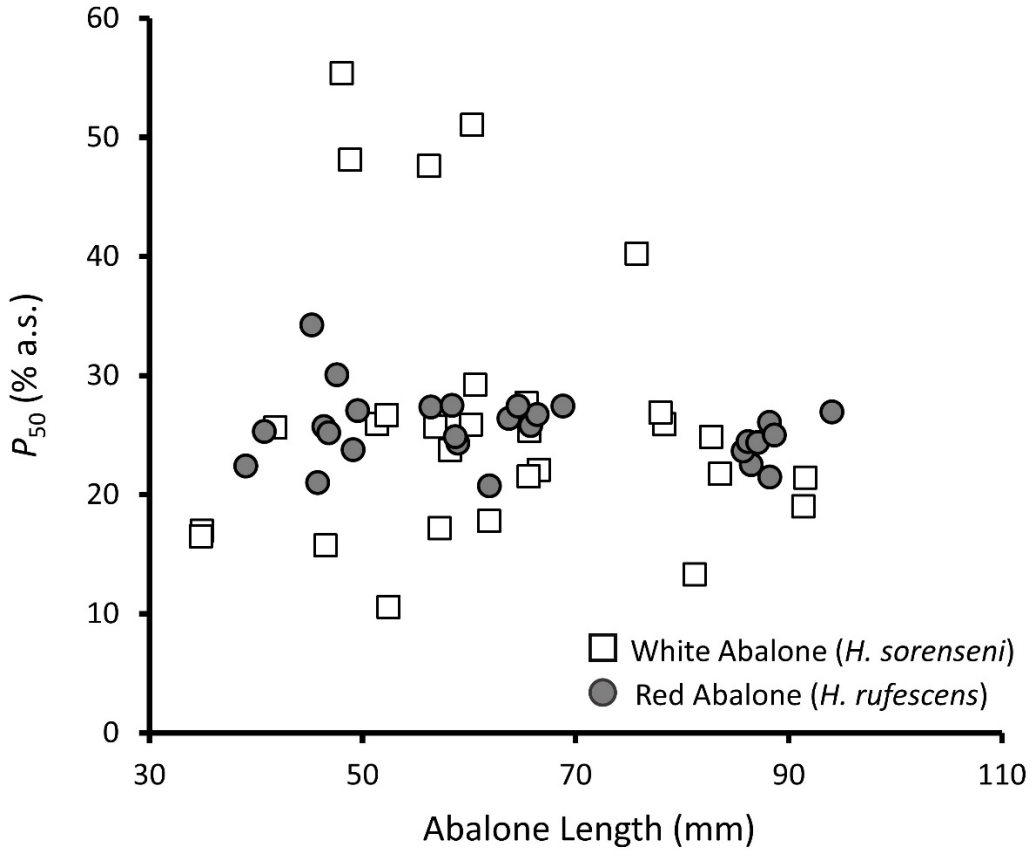

884

885 **Fig. S6.** Relationship between the P_{50} oxygen level (percent air saturation) and shell length
886 (mm) for white (*H. sorenseni,* n = 29) and red abalone (*H. rufescens,* n = 29) at 15°C.

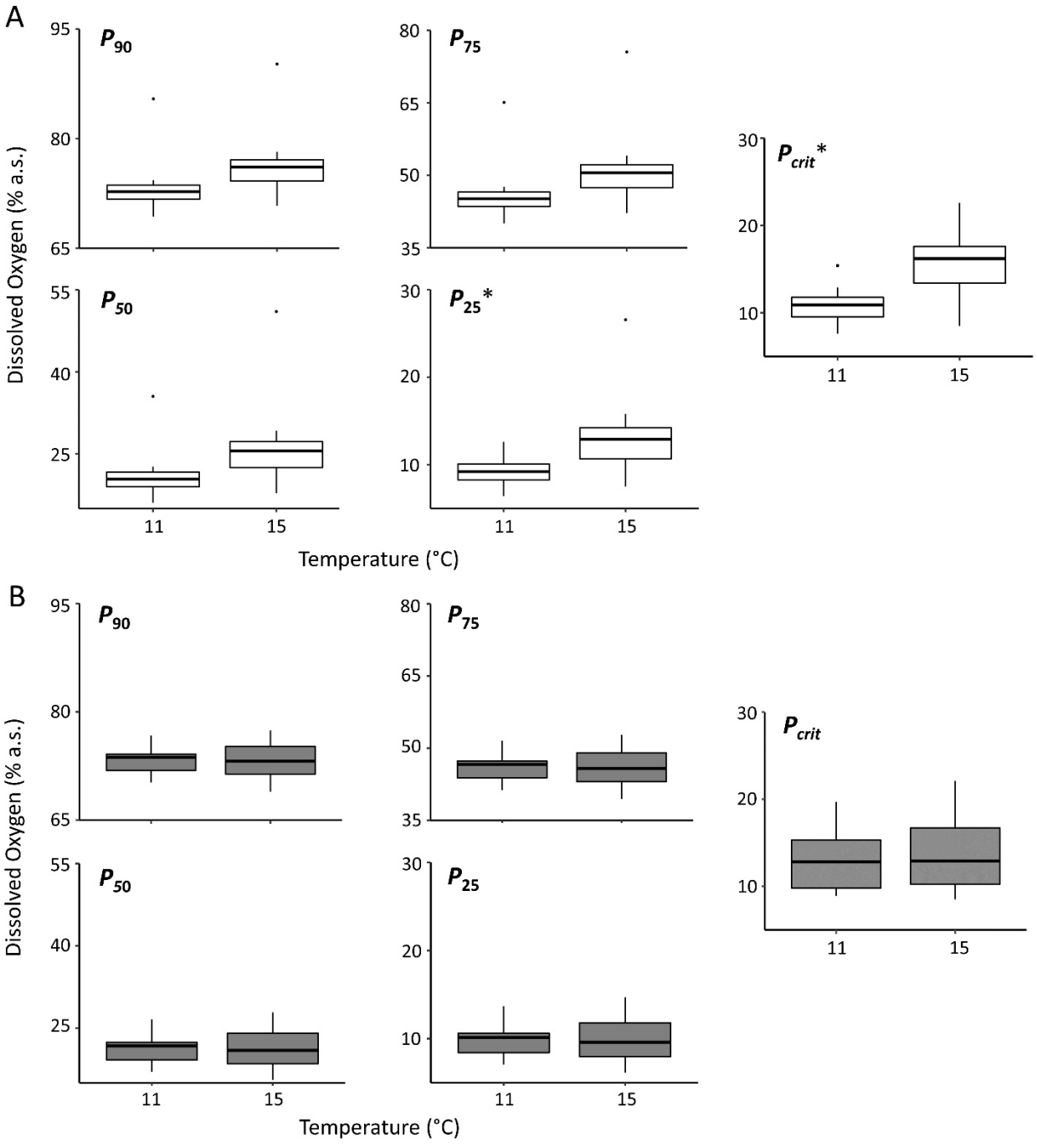

Fig. S7. Boxplots showing paired hypoxia tolerance measurements of P_{90}, P_{75}, P_{50}, P_{25}, and P_{crit} (dissolved oxygen level in percent air saturation) at both 11°C and 15°C for a subset of (A) white abalone (*H. sorenseni*, n=10) and (B) red abalone (*H. rufescens*, n=12). See Table 2 for details. *Indicates significant differences between temperatures.

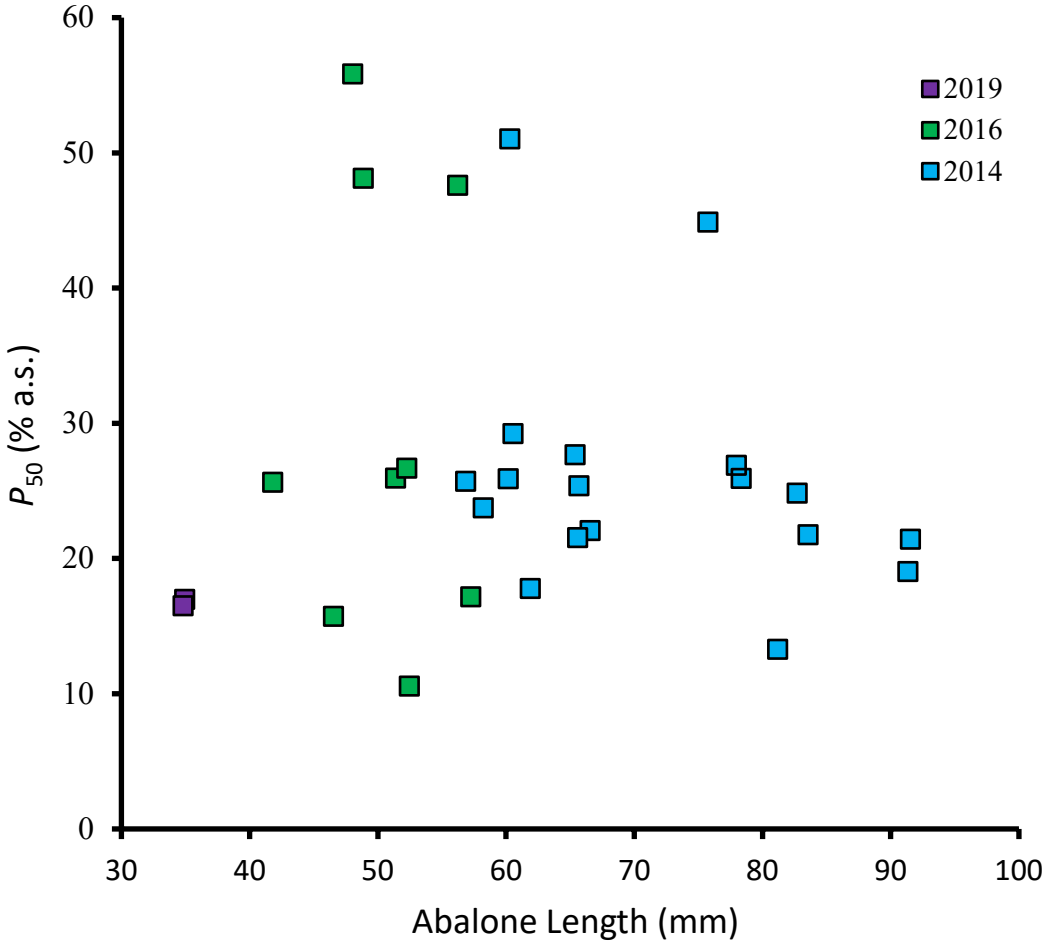

892

893 **Fig. S8.** Relationship between the P_{50} oxygen level (percent air saturation) and shell length
894 (mm) for white abalone (*H. sorenseni,* n = 29) at 15°C separated by cohort year (2014, 2016,
895 2019).
896

897

898

899

900

901

902

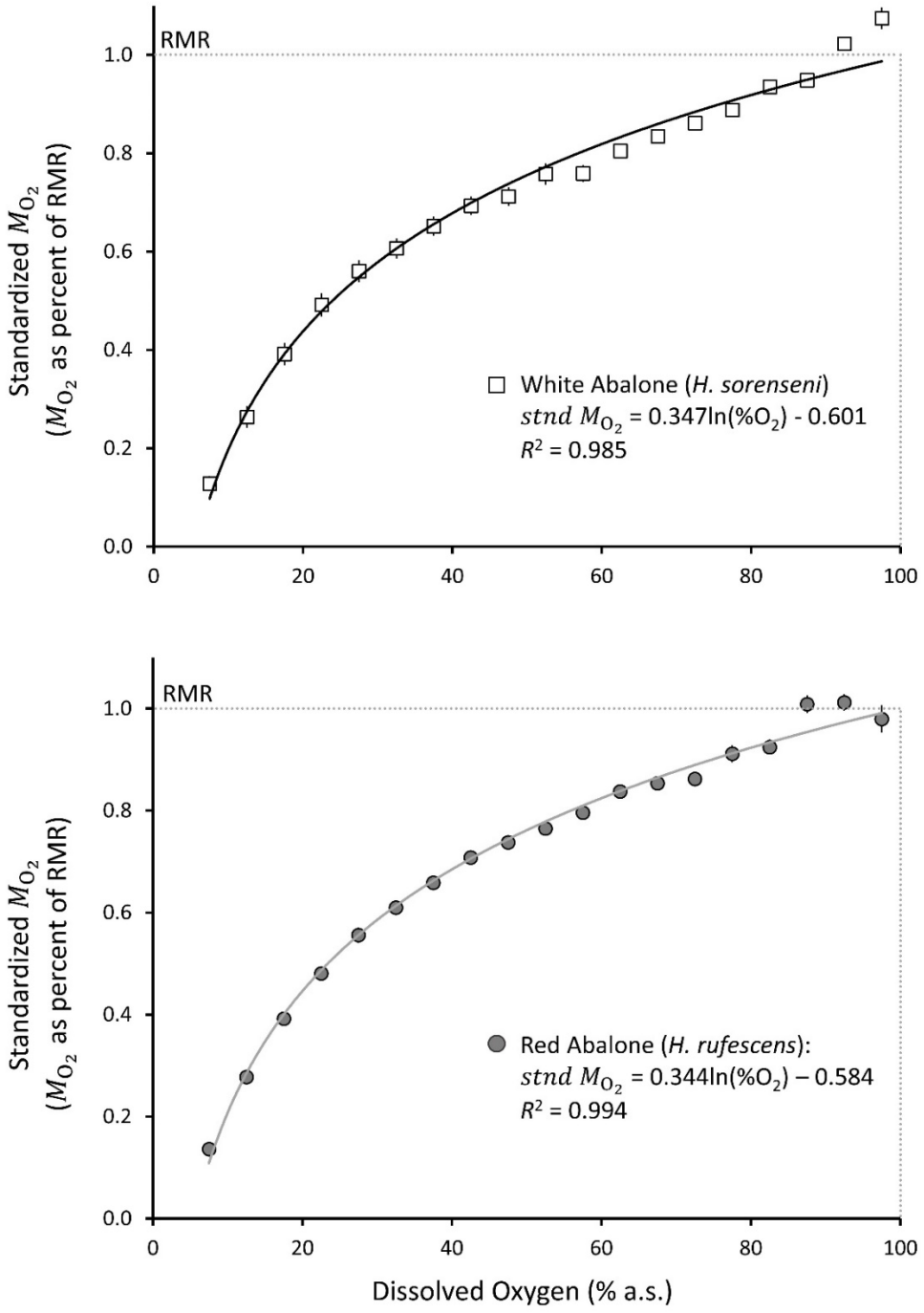

Fig. S9. Mean oxygen consumption rate (M_{O_2}) in relation to environmental dissolved oxygen (% air saturation) for white (*H. sorenseni*, n = 29) and red abalone (*H. rufescens*, n = 29) at 15°C from Fig. 3, standardized as a percent of total resting metabolic rate. Lines show best-fit logarithmic functions, and error bars show standard error of the mean. All *H. sorenseni* and *H. rufescens* data were scaled to a common total body mass of 40 g.